water

MDPI

Article

Ecological and Health Risk Assessment of Heavy Metals in Groundwater within an Agricultural Ecosystem Using GIS and Multivariate Statistical Analysis (MSA): A Case Study of the Mnasra Region, Gharb Plain, Morocco

Hatim Sanad [1,2,*], Rachid Moussadek [3], Houria Dakak [2], Abdelmjid Zouahri [2], Majda Oueld Lhaj [1,2] and Latifa Mouhir [1]

[1] Laboratory of Process Engineering and Environment, Faculty of Science and Technology Mohammedia, University Hassan II of Casablanca, Mohammedia 28806, Morocco; majdaoueldlhaj1999@gmail.com (M.O.L.); latifa.mouhir@fstm.ac.ma (L.M.)
[2] Research Unit on Environment and Conservation of Natural Resources, Regional Center of Rabat, National Institute of Agricultural Research, Av. Ennasr, Rabat 10101, Morocco; houria.dakak@inra.ma (H.D.); abdelmjid.zouahri@inra.ma (A.Z.)
[3] International Center for Agricultural Research in the Dry Areas (ICARDA), Rabat 10100, Morocco; r.moussadek@cgiar.org
* Correspondence: hatim.sanad99@gmail.com

Abstract: Assessing groundwater quality is essential for ensuring the sustainability of agriculture and ecosystems. This study evaluates groundwater contamination by heavy metals (HMs) using GIS approaches, multivariate statistical analysis (MSA), pollution indices (heavy metal pollution index (HPI), metal index (MI), degree of contamination (C_d), ecological risk index (ERI), and pollution index (PI)), and human health risk assessment (HHRA). The results revealed significant variations in heavy metal concentrations across the study area, with the highest concentrations found in the southern and southeastern parts, characterized by intense agricultural activities and uncontrolled landfills. Statistical analyses indicated both natural and anthropogenic sources of contamination. Pollution indices showed medium to high water pollution levels, with HPI values ranging from 20.23 to 128.60, MI values from 3.34 to 12.17, and Cd values from 2.90 to 11.73, indicating varying degrees of contamination. ERI values suggested a low ecological risk across all samples. However, health risk assessments highlighted significant non-carcinogenic and carcinogenic risks, particularly for children, with TCR values for some heavy metals like Ni and Cr exceeding safe limits, indicating potential health hazards. The findings provide a valuable framework for policymakers to develop targeted strategies for mitigating groundwater contamination and ensuring sustainable water quality management.

Keywords: groundwater quality; agriculture activities; heavy metals contamination; human health risk; ecological risk assessment; pollution indices; GIS techniques; statistical analysis; Morocco

check for updates

Citation: Sanad, H.; Moussadek, R.; Dakak, H.; Zouahri, A.; Oueld Lhaj, M.; Mouhir, L. Ecological and Health Risk Assessment of Heavy Metals in Groundwater within an Agricultural Ecosystem Using GIS and Multivariate Statistical Analysis (MSA): A Case Study of the Mnasra Region, Gharb Plain, Morocco. *Water* **2024**, *16*, 2417. https://doi.org/10.3390/w16172417

Academic Editors: Pietro Mazzon, Marco Taussi, Matteo Antelmi, Silvio Coda and Vincenzo Allocca

Received: 31 July 2024
Revised: 19 August 2024
Accepted: 23 August 2024
Published: 27 August 2024

Copyright: © 2024 by the authors. Licensee MDPI, Basel, Switzerland. This article is an open access article distributed under the terms and conditions of the Creative Commons Attribution (CC BY) license (https://creativecommons.org/licenses/by/4.0/).

1. Introduction

Water resources are essential for sustaining ecosystem balance and fostering the harmonious development of human society, the environment, and the economy [1]. Although water covers approximately 70% of the Earth's surface, less than 3% of this is freshwater, with only a small fraction—merely one-hundredth of a percent—suitable for human consumption [2–4].

Groundwater, which constitutes approximately 97% of the global supply of drinking water, is a primary freshwater source, valued for its widespread availability, safety, and purity [5–7]. Approximately 2.5 billion people globally rely exclusively on groundwater for their daily drinking needs [8]. Additionally, groundwater plays a significant role in

providing water for agricultural and industrial purposes, with about 43% of agricultural water sourced from it [9–12]. However, its quality is deteriorating worldwide due to intense anthropogenic activities such as increasing urbanization, poor management, excessive consumption, industrialization, agriculture, and exploitation of natural resources [13–15]. Numerous studies have demonstrated that anthropogenic activities lead to water resource pollution by HMs [16–18]. Globally, groundwater contamination by HMs is regarded as a critical environmental concern [19–21].

Metal contamination can arise from direct atmospheric precipitation, geological weathering, or the discharge of agricultural pesticides, fertilizers, and municipal, domestic, or industrial waste products [22–24]. The solubility of metals in soil and water is primarily influenced by pH, metal concentration, organic carbon content, ion exchange capacity, oxidation state of mineral components, and the system's redox potential [25,26]. Due to their stability, bioaccumulation in animal and plant tissues, and non-biodegradability, HMs persist in the environment, particularly in groundwater, resulting in ecological impacts and health problems [27–29]. HMs are metallic elements with high density and toxicity at certain concentrations [30]. Prolonged accumulation of HMs can significantly deteriorate health [31]. While metals such as copper (Cu), zinc (Zn), manganese (Mn), and iron (Fe) are essential micronutrients, they become toxic at higher concentrations [32]. In contrast, HMs like chromium (Cr), lead (Pb), mercury (Hg), cadmium (Cd), arsenic (As), nickel (Ni), fluorine (F), and cobalt (Co) offer no beneficial effects and can cause severe disruptions in bodily functions with long-term exposure [33,34]. Human exposure to HMs occurs through inhalation of polluted air, ingestion of contaminated food and water, and dermal contact with contaminated soil or water [35,36]. The adverse health effects of prolonged exposure to HMs include various cancers, mental retardation, neurological and cardiovascular disorders, kidney damage, developmental delays, poisoning, skin abnormalities, and bone diseases [37–40].

Groundwater risk assessment, grounded in monitoring results, is crucial for safeguarding groundwater resources. Monitoring HM concentrations is essential to avoid health implications and to determine the extent of pollution and its impact on health and ecosystems. Index approaches are particularly effective for evaluating groundwater quality in areas impacted by pollution, as they employ various indicators tailored to assess the concentration of metals in water [41]. For instance, the HPI is a valuable tool for calculating the collective pollution effect of HMs, assessing overall water quality, and determining suitability for human consumption [42–45]. Other indices, such as the heavy metal evaluation index (HEI), the Nemerow index (NeI), and the ERI for heavy metals in groundwater, provide similar assessments [46–48]. The MI considers the cumulative effects of trace elements, facilitating a rapid evaluation of overall water quality [45]. The C_d assesses the degree of pollution impacts on water quality based on specific trace elements [49]. Additionally, the PI assesses the relative toxicity of specific metals, providing a measure of their collective impact on water quality and contamination levels [50]. This index quantifies the extent of pollution caused by trace elements by accounting for the cumulative effects of individual contamination parameters that are considered detrimental to the environment [51,52].

Assessing HHRA is essential for evaluating the adverse impacts and potential health hazards posed to both ecosystems and human populations [53]. This assessment method is essential for identifying potential negative outcomes for individuals exposed to risk factors, particularly those linked to water sources with high contaminant concentrations [54]. Health risk assessments evaluate the current health status and future illness or mortality risks for individuals consuming or exposed to contaminated groundwater [55]. These evaluations differentiate between non-carcinogenic and carcinogenic risks by considering the varying toxicological profiles of the chemical elements involved [56]. Variations in factors such as age, weight, dietary habits, and the selection of parameters introduce considerable uncertainty in the assessments [14]. The overall quality of water can be evaluated through the measurement of chronic daily intake (CDI), whereas non-carcinogenic health risks

linked to the consumption of water contaminated with metals are typically assessed using the hazard quotient (HQ) and hazard index (HI) [57,58].

Numerous investigations have focused on variations in heavy metal concentrations in groundwater and their associated health risks across diverse geographical regions [59,60]. For instance, Dippong et al. [61] assessed groundwater contamination and associated risk factors in Romania's north-west region by applying various pollution and risk indices. In Togo, Toi Bis-sang et al. [16] carried out a comprehensive analysis of heavy metal pollution and potential health risks at a former iron mining site, utilizing HPI and HHRA. Rashid et al. [62] similarly examined groundwater quality, health risks, and contamination patterns surrounding chromite mining areas through HHRA. Liu et al. [63] addressed heavy metal contamination and health risks in Wuhan's tap water, employing HPI to propose strategies for enhancing urban water supply security and addressing sustainability issues. Furthermore, Egbueri et al. [64] evaluated drinking water quality in Ojoto and nearby areas using the pollution index of groundwater (PIG), ERI, and hierarchical cluster analysis (HCA).

Multivariate statistical approaches (MSAs), including correlation analysis (CA), principal component analysis (PCA), and HCA, are commonly utilized to understand the mechanisms affecting groundwater quality [65–67]. Recently, GIS techniques, combined with the inverse distance weighting (IDW) interpolation method, have been employed for assessing and monitoring groundwater quality. This methodology has demonstrated considerable efficacy in analyzing and interpreting spatial data associated with water resources [68].

The primary objectives of this exploratory research are twofold: first, to elucidate the variations in concentration and spatial distribution of HMs in groundwater across the Mnasra region in the Gharb Plain using MSA and key indicators such as HPI, MI, Cd, ERI, and PI, supplemented by a GIS approach; second, to estimate the potential health risks associated with heavy metal exposure by evaluating both non-carcinogenic and carcinogenic risks for adults and children.

2. Materials and Methods

2.1. Description of the Study Area

The study was carried out in the Mnasra region, situated in the Gharb Plain, a prominent agricultural zone along the Atlantic coast, encompassing an area of 488 km^2 (Figure 1). This region extends from Kenitra in the south to the Sebou River, bounded by a line that runs through Sidi Allal Tazi to the east and reaches Merja Zerga near Moulay Bousselham in the north.

The Mnasra region is influenced by a Mediterranean climate, exhibiting significant oceanic effects. This climatic setting results in an average annual rainfall of around 551 mm. Temperature variations are distinct, with winter temperatures averaging around 12 °C and summer temperatures reaching up to 23 °C. Additionally, potential evaporation rates are notably high, exceeding 150 mm between June and September, but decrease to below 80 mm during the winter months from December to February.

Geologically, the coastal zone of the region is predominantly covered by sandy soils, which account for around 39,000 hectares, or 15% of the total area. The area itself is distinguished by its sandy-clay and silty-clay soil textures.

The Sebou River, a major watercourse in the Gharb region, predominantly shapes the area's hydrological network. This influential river is complemented by several key tributaries, such as the Ouerrha, Beht, Rdom, and Tiflet rivers, which collectively contribute to the region's hydrological dynamics. Aquifer recharge primarily occurs through rainwater infiltration and the return flow from irrigation. The prevailing flow direction in the southern part of the plain is from southeast to northwest, shifting to an east–west direction in the central and western areas.

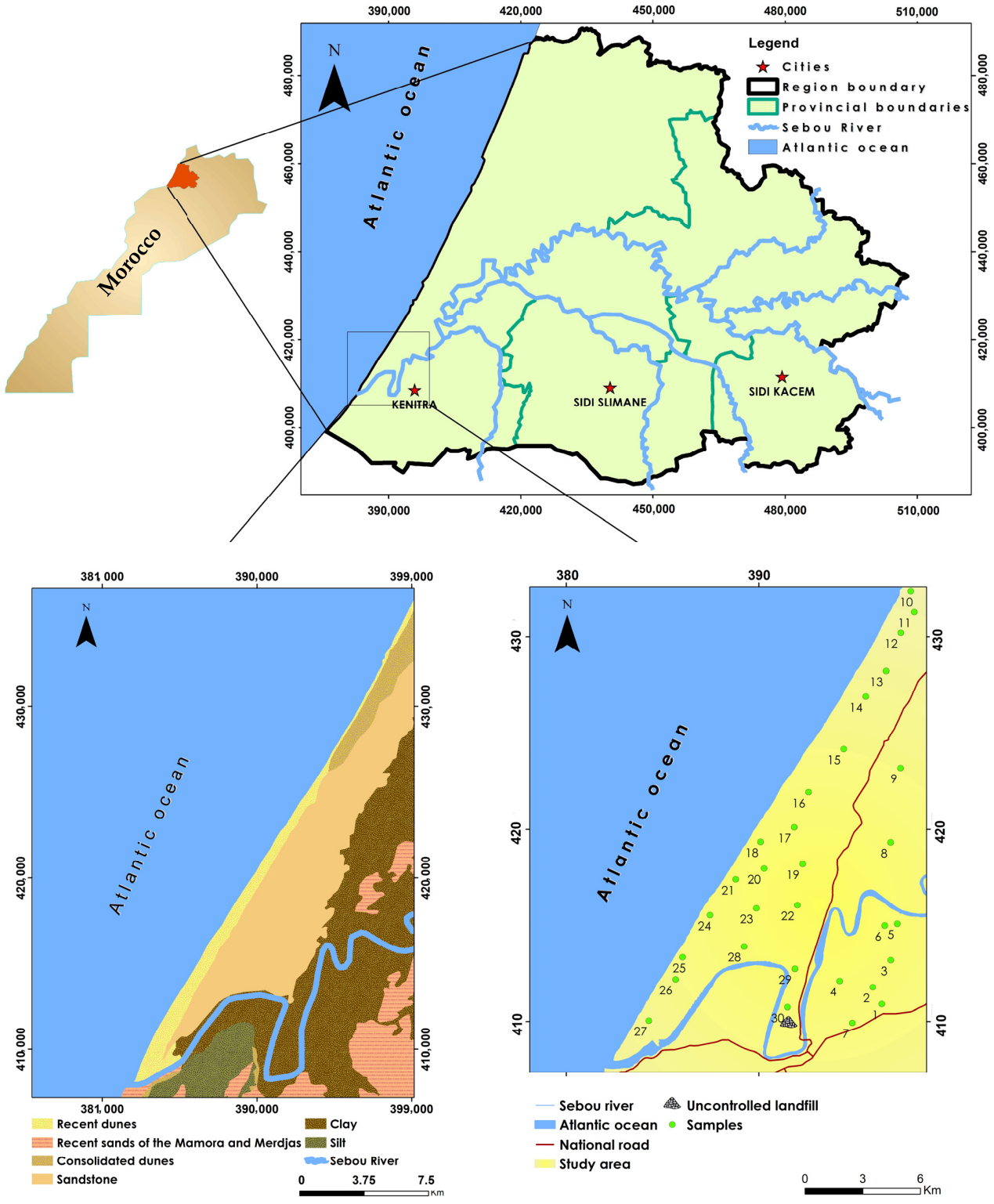


Figure 1. Map of the study site and measurement stations.

The Mnasra region, widely recognized for its sugarcane cultivation, plays a pivotal role in Morocco's sugar industry. The agricultural activities in this region encompass not only extensive sugarcane farming but also involve intensive cultivation of vegetables, field crops, and tree crops [69]. These farming activities often incorporate both mineral and organic fertilizers, including ammonium nitrate, NPK blends, urea, as well as manure from cattle and poultry.

Additionally, the uncontrolled landfill at "Ouled Berjal" is located within the urban perimeter of the study area, 3 km north of the Kenitra conurbation, in a loop of the Sebou River that surrounds it on the east, south, and west sides. This landfill covers over 20 hectares and receives an average of 510 tons of waste per day, totaling 186,000 tons annually [70]. The waste exhibits significant typological variability, reflecting the agricultural, industrial, and artisanal activities of the region.

2.2. Sampling Collection and Analysis

In the present study, thirty groundwater samples were collected in March 2024 from diverse sites within the defined study zone (Figure 1). Sampling locations were strategically selected at consistent intervals, taking into account local geographical features and prioritizing areas associated with high-intensity agricultural activities, notable geological characteristics, and closeness to a landfill. The chosen wells cater to both agricultural and residential needs.

To avoid any risk of cross-contamination, polyethylene sampling bottles (500 mL) were pre-cleaned with distilled water and subsequently rinsed three times with the local sample water before collection. The water samples were then gathered and transported in insulated coolers, ensuring a consistent temperature of 4 °C until they reached the laboratory for analysis. Upon collection, groundwater samples were divided into two sets. For the measurement of total metal content, one set of samples was acidified with 0.5% nitric acid before filtration through 0.45 µm filter paper. For the determination of dissolved metal content, a separate set of samples was first filtered through 0.45 µm filter paper and then acidified with 0.5% nitric acid [71].

HM concentrations for ten elements (As, Cd, Cr, Cu, Fe, Hg, Mn, Ni, Pb, and Zn) were analyzed using inductively coupled plasma mass spectrometry (ICP-MS) (Agilent 7800 ICP-MS, Santa Clara, CA, USA) [72]. This sophisticated technique provides precise quantification of heavy metals, thereby improving the accuracy and reliability of the analytical results.

2.3. Multivariate Statistical Analysis

Descriptive statistics for each parameter were analyzed using IBM SPSS Statistics 25, encompassing measures such as minimum, maximum, mean, variance, standard deviation, coefficient of variation (CV), skewness, and kurtosis. These statistics provided a detailed summary of the dataset. To evaluate the relationships between different sample attributes, Pearson correlation coefficients were calculated. The PCA was utilized to distill the dataset into principal components (PCs), addressing multicollinearity and enhancing the clarity of the data representation by reducing the dimensionality of heavy metal concentration data [73]. In addition, HCA with Ward's linkage method was applied to classify variables into distinct clusters, uncovering potential associations among heavy metals in groundwater samples.

Spatial distribution was mapped using GIS techniques and contouring methods in ArcGIS 10.6. The inverse distance weighting (IDW) interpolation technique was employed to create these maps, visualizing spatial variations across the study area. IDW, a fundamental and extensively used interpolation method, facilitated the calculation of heavy metal concentrations based on statistical relationships between known locations [74].

2.4. Pollution Evaluation Indices

2.4.1. Heavy Metal Pollution Index (HPI)

The HPI is a valuable tool for evaluating the degree and effects of different HMs on water quality [75,76]. To determine the contamination levels in groundwater, appraisal scores were derived using a weighted arithmetic mean [77]. In this analysis, weights were assigned between 0 and 1 for each metal based on its relative importance in drinking water, with measurable limits for the standard permitted value (Si) and ideal value (Ii) provided by the World Health Organization (WHO) [78], as detailed in Table 1.

Table 1. The WHO (2017) guidelines of HMs and weight scores.

Parameters	Si (µg/L)	Wi	MACi (µg/L)
As	10	0.1349614	10
Cd	3	0.4498715	30
Cr	50	0.0269923	50
Cu	2000	0.0006748	2000
Fe	300	0.0044987	300
Hg	6	0.2249357	6
Mn	400	0.003374	400
Ni	70	0.0192802	70
Pb	10	0.1349614	10
Zn	3000	0.0004499	3000
Total		1	

HPI values were calculated according to Equation (1), as follows:

$$\mathrm{HPI} = \frac{\sum_{i=1}^{n} \mathrm{Wi} \times \mathrm{Qi}}{\sum_{i=1}^{n} \mathrm{Wi}} \quad (1)$$

where "Wi" is the unit weight of the ith parameter, and "Qi" is the sub-index of the ith parameter, which are calculated using Equations (2) and (3):

$$\mathrm{Wi} = \frac{\mathrm{k}}{\mathrm{Si}} \quad (2)$$

where "k" is the proportionality constant and "Si" is the ith the authorized standard value.

$$\mathrm{Qi} = \sum_{i=1}^{n} \frac{(\mathrm{Ci} - \mathrm{Ii})}{(\mathrm{Si} - \mathrm{Ii})} \times 100 \quad (3)$$

where "Ci" represents the monitored value of the heavy metal, "Ii" is the ideal value, and "Si" is the standard permissible value set by WHO.

The classification of waters based on HPI includes three categories, as shown in Table 2.

Table 2. Classification of the HPI [79].

HPI Values	HPI Classification
<15	Low water pollution
15 < HPI < 30	Medium water pollution
>30	High water pollution

2.4.2. Metal Index (MI)

The MI is a widely used method for evaluating the global quality of water with respect to metal content [41]. This index offers a broad assessment of the current status of water quality, allowing for trend analysis over time [45,80]. The MI is determined by calculating the ratio of the concentration of each metal in the water to its corresponding maximum allowable concentration (MACi) (Table 1). The MI can be calculated using Equation (4), as follows:

$$\mathrm{MI} = \sum_{i=1}^{n} \frac{\mathrm{Ci}}{\mathrm{MACi}} \quad (4)$$

where "Ci" is the measured concentration of the ith parameter, "MACi" is the maximum permitted value for each metal, and "i" is the ith sample.

The total values were divided into six classes, indicating groundwater pollution [81]. The list is shown in Table 3.

Table 3. Classification of the MI.

MI Values	MI Classification
<0.3	Very pure
0.3 < MI < 1	Pure
1 < MI < 2	Slightly affected
2 < MI < 4	Moderately affected
4 < MI < 6	Strongly affected
>6	Seriously affected

2.4.3. Degree of Contamination (C_d)

The quality of groundwater is evaluated by determining the C_d, which gives a combined effect of contamination due to individual elements considered harmful. The C_d is calculated and measured based on the contamination factors of specific trace elements that exceed acceptable limits [82], according to Equations (5) and (6):

$$C_d = \sum_{i=1}^{n} C_{fi} \quad (5)$$

$$C_{fi} = \frac{C_{Ai}}{C_{Ni}} - 1 \quad (6)$$

where "C_{fi}" is the contamination factor of the ith component, "C_{Ai}" is the analytical value of the ith component, "C_{Ni}" is the maximum permissible concentration of ith component, with reference to the MAC (Table 1).

The resultant C_d value identifies areas of varying contamination levels, which are grouped into three categories as indicated in Table 4.

Table 4. Classification of the C_d [83].

C_d Values	C_d Classification
<1	Low
1 < C_d < 3	Medium
>3	High

2.4.4. Ecological Risk Index (ERI)

The ERI provides a quantitative measure of the potential ecological risk posed by the presence of HMs in groundwater [84]. This method helps in assessing the combined impact of multiple metals, taking into account both their concentrations and their relative toxicities [85]. The potential ERI of the analyzed heavy metals was quantitatively evaluated by considering their pollution index and toxic-response factor using Equations (7) and (8), as follows:

$$\text{ERI} = \sum_{i=1}^{n} \text{RI} = \sum_{i=1}^{n} \text{Ti} \times \text{PI} \quad (7)$$

$$\text{PI} = \frac{C_s}{C_b} \quad (8)$$

where "RI" is the potential ecological risk factor of the ith heavy metal; "Ti" is the toxic-response factor for the ith heavy metal; "PI" is the pollution index for the ith heavy metal; "C_s" is the concentration of heavy metals in the sample; and "C_b" is the corresponding background values. The toxic-response factor of heavy metals is given as Cd 30; As 10; Cu, Hg, Ni, and Pb 5; Fe, Cr, Zn, and Mn 1 [64].

The ERI values are classified into four groups (Table 5).

Table 5. Classification of the ERI [86].

ERI Values	ERI Classification
<150	Low ecological risk
150 < ERI < 300	Moderate ecological risk
300 < ERI < 600	Considerable ecological risk
>600	Very high ecological risk

2.4.5. Pollution Index (PI)

The impact of trace elements on water quality was evaluated through the calculation of PI values. These values, which are derived from the concentrations of individual metals, allow for the classification of contamination into five distinct categories, as shown in (Table 6) [82,87].

Table 6. Classification of the PI.

PI Values	PI Classification
<1	No effect
1 < PI < 2	Slightly affected
2 < PI <3	Moderately affected
3 < PI <5	Strongly affected
>5	Seriously affected

The PI values were calculated using Equation (9), as follows:

$$PI = \frac{\sqrt{\left(\frac{Ci}{Si}\right)^2_{Max} + \left(\frac{Ci}{Si}\right)^2_{Min}}}{2} \quad (9)$$

where "Ci" is the metal concentration and "Si" is the metal level in relation to the metal concentration in water.

2.5. Human Health Risk Assessment (HHRA)

Consumption of drinking water contaminated with toxic metals increases the risk of non-carcinogenic and carcinogenic diseases in humans [88,89]. The HHRA associated with HMs in tap water was carried out using the model established by the United States Environmental Protection Agency (US EPA) [90]. Exposure determination involves estimating the daily exposure value of the human body to HMs [91]. Key exposure routes include direct ingestion, inhalation, and dermal absorption [92]. The assessment computes the pollutant dose consumed by humans using chronic daily intake (CDI), which reflects the dose of pollutants in kilograms per day absorbed through direct ingestion (CDI_i) and dermal absorption (CDI_d) for both adults and children using Equations (10) and (11) [63]:

$$CDI_i = \frac{(C_i \times IR \times EF \times ED)}{(BW \times AT)} \quad (10)$$

$$CDI_d = \frac{(C_i \times SA \times k_p \times ET \times EF \times ED \times CF)}{(BW \times AT)} \quad (11)$$

where CDI_i (µg/kg/day) and CDI_d (µg/kg/day) are the chronic daily intake doses through ingestion and dermal absorption of water, respectively. In Equations (10) and (11), "C_i" is the concentration of the HM (µg/L), "K_p" is the dermal permeability coefficient (cm/h) of heavy metal in water, "IR" is the ingestion rate, "EF" represents exposure frequency, "ED" is exposure duration, "BW" indicates body weight, "AT" is the average time for non-carcinogens, "SA" is the exposed skin area, "ET" represents exposure time, and "CF" is the conversion factor [16,93].

The non-carcinogenic risks were determined by applying the hazard quotient (HQ) [94] using Equations (12) and (13):

$$HQ_i = \frac{CDI_i}{R_fD_i} \quad (12)$$

$$HQ_d = \frac{CDI_d}{R_fD_d} \quad (13)$$

where "R_fD_i" and "R_fD_d" are the ingestion and oral/dermal reference doses (mg/kg/day), respectively [95,96]. The "HQ_i" is the hazard quotient through ingestion, and "HQ_d" is the hazard quotient through dermal absorption.

The summation of the non-carcinogenic risk of an individual HM is presented as a hazard index (HI) for the two exposure routes, and computed following Equation (14), as follows:

$$HI = HQ_i + HQ_d \quad (14)$$

This index categorizes health risks into two types: HI < 1 indicates a low detrimental impact of HMs on human health, while HI > 1 represents greater chances of harmful health effects [97].

The carcinogenic risks (CRs) of HMs were calculated to evaluate the chances of an individual developing cancer during their lifespan due to their contact with potential carcinogens. CR was computed using Equations (15) and (16), as follows:

$$CR_i = CDI_i \times CSF \quad (15)$$

$$CR_d = CDI_d \times CSF \quad (16)$$

where CSF is the carcinogenic slope factor, a toxicity value that describes the association between dose and response. CSF (mg/kg/day) values are as follows: As = 1.5; Cr = 0.5; Cd = 15; Ni = 1.7; and Pb = 1.7 [98].

The total carcinogenic risk (TCR) was subsequently determined by summing the individual CR for each hazardous metal, as described in Equation (17):

$$TCR = CR_i \times CR_d \quad (17)$$

A TCR value less than 10^{-6} indicates a negligible carcinogenic risk, posing minimal concern for human health. When the TCR falls between 10^{-6} and 10^{-4}, it is considered an acceptable or tolerable risk, which suggests that while there may be some level of risk, it is within a range deemed manageable and generally safe. However, when the TCR exceeds 10^{-4}, it signals a high risk, indicating significant potential for adverse health effects, and necessitates urgent attention and possible intervention [99].

3. Results and Discussion

3.1. HMs Analysis and Spatial Variation

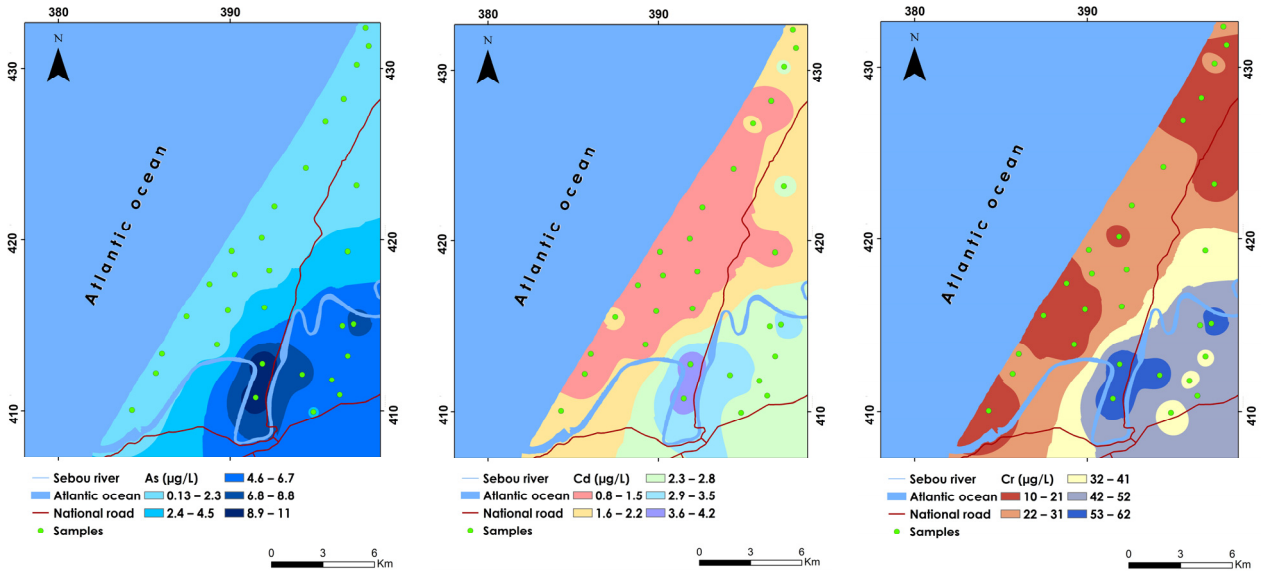
Descriptive statistics data for the studied heavy metal levels in groundwater samples are summarized in Table 7.

Arsenic (As), a naturally occurring element found in various environmental compartments, is significantly influenced by both natural processes and human activities such as mining, pesticide use, and agricultural practices involving arsenic-based additives [100]. In this study, As concentrations ranged from 0.13 to 11.02 µg/L, with a mean concentration of 3.01 µg/L and a standard deviation of 2.93, indicating moderate variability in its distribution across sampled sites (Table 7). The CV% of 0.97 indicates a relatively stable distribution of As in the groundwater across the study area. Notably, the highest recorded As concentration was found at sample P29, while the lowest was observed at sample P24, underscoring spatial variability in contamination levels. Notably, 6.66% of the samples, specifically P29 and P30, surpassed the WHO guideline limit of 10 µg/L. These

elevated concentrations, ranging between 8.9 and 11 µg/L, were predominantly found in the southern and southeastern regions of the study area (Figure 2a).

Table 7. Statistical results of HMs in groundwater samples.

Parameters	Unit	Minimum	Maximum	WHO (2017)	Mean	St. Dev.	CV	Skewness	Kurtosis
As	(µg/L)	0.13	11.02	10	3.01	2.93	0.97	1.57	1.61
Cd		0.80	4.20	3	1.86	0.95	0.51	1.01	0.04
Cr		10.30	62.00	50	29.01	15.89	0.55	0.89	−0.28
Cu		115.60	2289.60	2000	549.82	534.70	0.97	2.26	5.43
Fe		297.10	511.60	300	391.92	55.02	0.14	0.74	−0.28
Hg		0.10	6.20	6	1.35	1.79	1.33	1.83	2.24
Mn		126.40	689.60	400	304.76	112.85	0.37	1.86	4.86
Ni		25.60	76.10	70	44.98	15.05	0.33	0.65	−0.67
Pb		1.03	15.25	10	4.43	4.35	0.98	1.04	−0.29
Zn		1057.50	4525.40	3000	1727.51	904.38	0.52	1.64	2.45



(**a**) (**b**) (**c**)

Figure 2. Spatial distribution maps of (**a**) As, (**b**) Cd, and (**c**) Cr.

This spatial distribution pattern raises concerns for human health, as chronic exposure to elevated As levels through drinking water can pose significant health risks, including skin lesions, developmental effects, cardiovascular disease, and even cancer [101].

Cadmium (Cd), primarily originating from geogenic sources like minerals containing calcium and magnesium ions, also enters the environment through human activities such as battery processing, phosphate fertilizer use, and agrochemical applications containing Cd compounds [102]. The study revealed that Cd concentrations ranged from 0.8 to 4.20 µg/L, with a mean concentration of 1.86 µg/L and a relatively low standard deviation of 0.95, indicating moderate variability across sampled sites (Table 7). The Cd exhibited a CV% of 0.51, suggesting a consistent distribution pattern across the groundwater. Notably, the highest recorded Cd concentration was observed at sample P29, while the lowest was found at sample P23, demonstrating spatial variability in contamination levels (Figure 2b). Approximately 13.33% of samples (P4, P5, P29, and P30) exceeded the WHO guideline limit, highlighting areas of concern, particularly in the southern part of the study area where concentrations ranged between 3.6 and 4.2 µg/L. However, lower Cd concentrations were predominantly found in the western and central regions of the study area. This spatial distribution pattern can be attributed to extensive runoff from agricultural fields where

pesticides and phosphate fertilizers containing Cd are commonly used. Such agricultural practices intensify the risk of Cd leaching into groundwater, posing potential health hazards to local communities reliant on this water source [103].

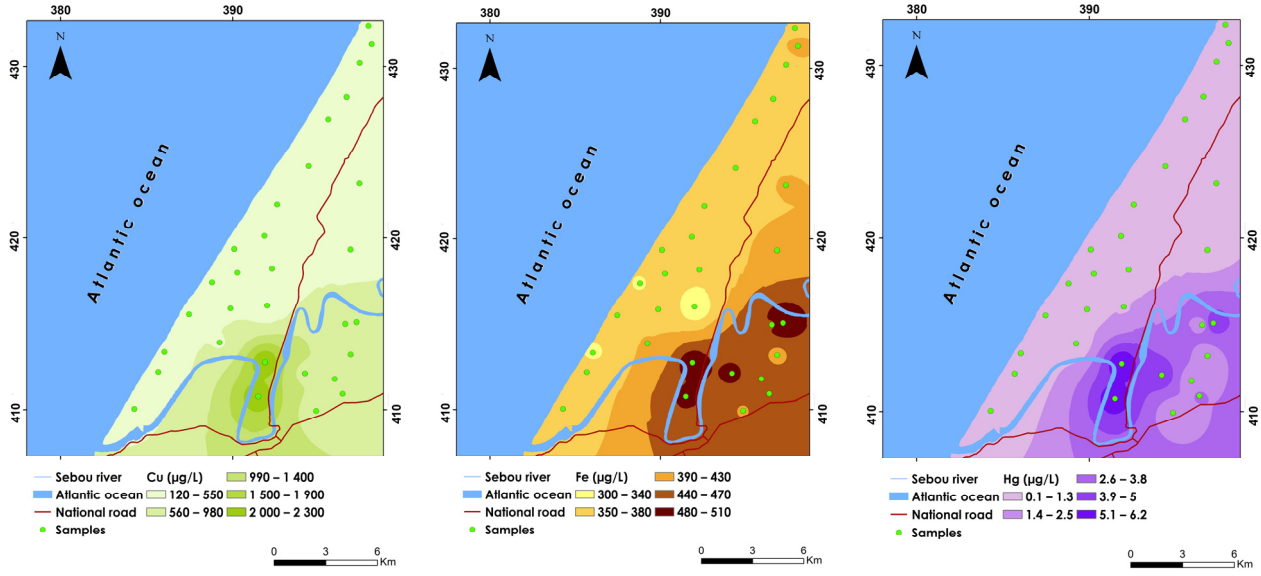
The presence of chromium (Cr) in groundwater is mainly linked to human activities, including the use of sewage sludge, wastewater discharge, metal and wood preservation, water cooling systems, and mining operations [104]. The Cr concentrations ranged from 10.3 to 62 µg/L, with a mean concentration of 29.01 µg/L and a standard deviation of 15.89, indicating substantial variability in the data (Table 7). The CV% of 0.55 reflects a moderate range of dispersion among the Cr concentration values. The highest concentration was observed at sample P29, whereas the lowest was found at sample P23. Notably, 13.33% of the groundwater samples, specifically samples P4, P5, P29, and P30, exceeded the WHO guideline limit of 50 µg/L. Spatial distribution analysis shows that the highest concentrations of Cr are located in the southern and southeastern parts of the study area, ranging between 53 and 62 µg/L (Figure 2c). Conversely, the lower concentrations are found in the western, central, and northern parts of the study site, with values lower than 21 µg/L. The elevated levels of Cr in the southern regions are likely attributed to extensive anthropogenic activities such as wastewater discharge, landfill leachates, and possibly improper disposal of chromium-containing substances [105]. In plants, chromium adversely affects growth and development by hindering the germination process and altering the growth patterns of leaves, roots, and stems [106]. These detrimental effects on plant health can lead to reduced agricultural productivity and compromised ecosystem stability [86].

Copper (Cu) is an essential nutrient for the human body, crucial for various physiological processes. However, excessive levels of drinking water can pose health risks [107]. The Cu concentrations ranged widely from 115.6 to 2289.6 µg/L, with a mean concentration of 549.82 µg/L and a standard deviation of 534.7, indicating considerable variability among samples (Table 7). The CV% of 0.97 underscores high dispersion levels across the study area. Sample P29 recorded the highest concentration, while sample P8 exhibited the lowest. Approximately 6.66% of the groundwater samples (P29 and P30) exceeded the WHO guideline limit of 2000 µg/L. Spatially, elevated Cu concentrations are predominantly found in the southern and southeastern parts of the study area, exceeding 1500 µg/L (Figure 3a). Conversely, lower concentrations are observed in the western, central, and northern parts, below 550 µg/L. The higher Cu levels in the southern regions may be attributed to agricultural activities such as pesticide use, where copper-based fungicides and bactericides are commonly applied. Moreover, industrial effluent sewage discharges can also contribute to elevated Cu levels in groundwater [108].

The concentrations of iron (Fe) in the groundwater samples ranged from 297.10 to 511.60 µg/L, with a mean concentration of 391.92 µg/L and a standard deviation of 55.02, indicating moderate variability in iron levels (Table 7). The CV% of 0.14 indicates a relatively low level of variability around the mean, reflecting a more uniform distribution of Fe concentrations across the study area. Despite this uniformity, all samples except for one (P22) exceeded the WHO guideline limit of 300 µg/L. The highest concentration was recorded at sample P5, while the lowest concentration, just below the WHO limit, was observed at sample P22. Spatial analysis reveals that the highest Fe concentrations, exceeding 480 µg/L, are primarily located in the southern and southeastern sections of the study area (Figure 3b). Conversely, lower concentrations, below 340 µg/L, were identified in the western and central regions.

The mercury (Hg) levels in the sampled groundwater ranged from 0.10 to 6.20 µg/L, with an average concentration of 1.35 µg/L and a standard deviation of 1.79 µg/L, indicating considerable variability (Table 7). The CV% of 1.33 suggests significant dispersion around the mean, reflecting heterogeneous distribution patterns of Hg concentrations across the study area. Despite the variability, it is noteworthy that nearly all samples, except for one (P29), were below the WHO guideline limit of 6 µg/L. The highest mercury concentration was recorded at sample P29, while the lowest concentrations, below 1.3 µg/L,

were observed at samples P10, P12, P26, and P27. The spatial distribution of Hg shows the highest concentrations predominantly in the southern part of the study area, with values ranging from 5.1 to 6.2 µg/L (Figure 3c). In contrast, lower values were found in the central, northern, and western parts, indicating a spatial pattern that may be influenced by local sources of Hg contamination. The Hg contamination in groundwater can stem from both natural and anthropogenic sources, including the use of mercury in agricultural chemicals, landfill leachate, and improper waste disposal [109].



(**a**) (**b**) (**c**)

Figure 3. Spatial distribution maps of (**a**) Cu, (**b**) Fe, and (**c**) Hg.

Manganese (Mn) is primarily introduced into groundwater through the suspension of manganese oxides and manganese-containing carbonate minerals [110]. Additionally, human activities such as industrial processes and agricultural practices, including the use of fungicides, fertilizers, and pesticides, contribute to Mn contamination [23]. The Mn concentrations ranged from 126.40 to 689.60 µg/L, with an average concentration of 304.76 µg/L and a standard deviation of 112.85 µg/L, indicating a moderate stage of variability (Table 7). The CV% of 0.37 suggests that while there is some dispersion around the mean, the distribution of Mn concentrations is relatively consistent across the study area. The highest Mn concentration was recorded at sample P29, while the lowest was at sample P7. The spatial distribution showed that the highest values were predominantly located in the southern and southeastern parts of the study area, ranging between 470 and 690 µg/L (Figure 4a).

The WHO recommends a maximum permissible limit of 400 µg/L for Mn in drinking water. The results show that 6.66% of the samples (P29 and P30) exceeded this limit, indicating potential health risks. Excessive Mn intake can lead to neurological and psychological issues [111].

Nickel (Ni) is a naturally occurring element found in trace quantities within the earth's crust, leading to its presence in food, water, soil, and air as a result of natural processes [112]. The concentrations of Ni ranged from 25.60 to 76.10 µg/L, with a mean value of 44.98 µg/L and a standard deviation of 15.05 µg/L (Table 7). The CV% was 0.33, indicating a moderate variation in Ni concentrations across the samples. The highest concentration was recorded at sample P29, while the lowest was at sample P23. The spatial analysis reveals that the highest values were found in the southern and southeastern parts of the study area, with concentrations ranging from 67 to 76 µg/L (Figure 4b). In contrast, the lower concentrations were observed in the western and central parts of the study area, with values below 36 µg/L. Approximately 13.33% of the samples (P4, P5, P29, and P30) exceeded the WHO limit of

70 µg/L. The elevated levels of Ni in these areas are likely influenced by anthropogenic activities, such as the extensive use of phosphate fertilizers and sewage disposal, which can increase nickel concentrations in groundwater [113]. High Ni concentrations can lead to soil contamination, adversely affecting plant health and potentially altering the overall ecosystem [61].

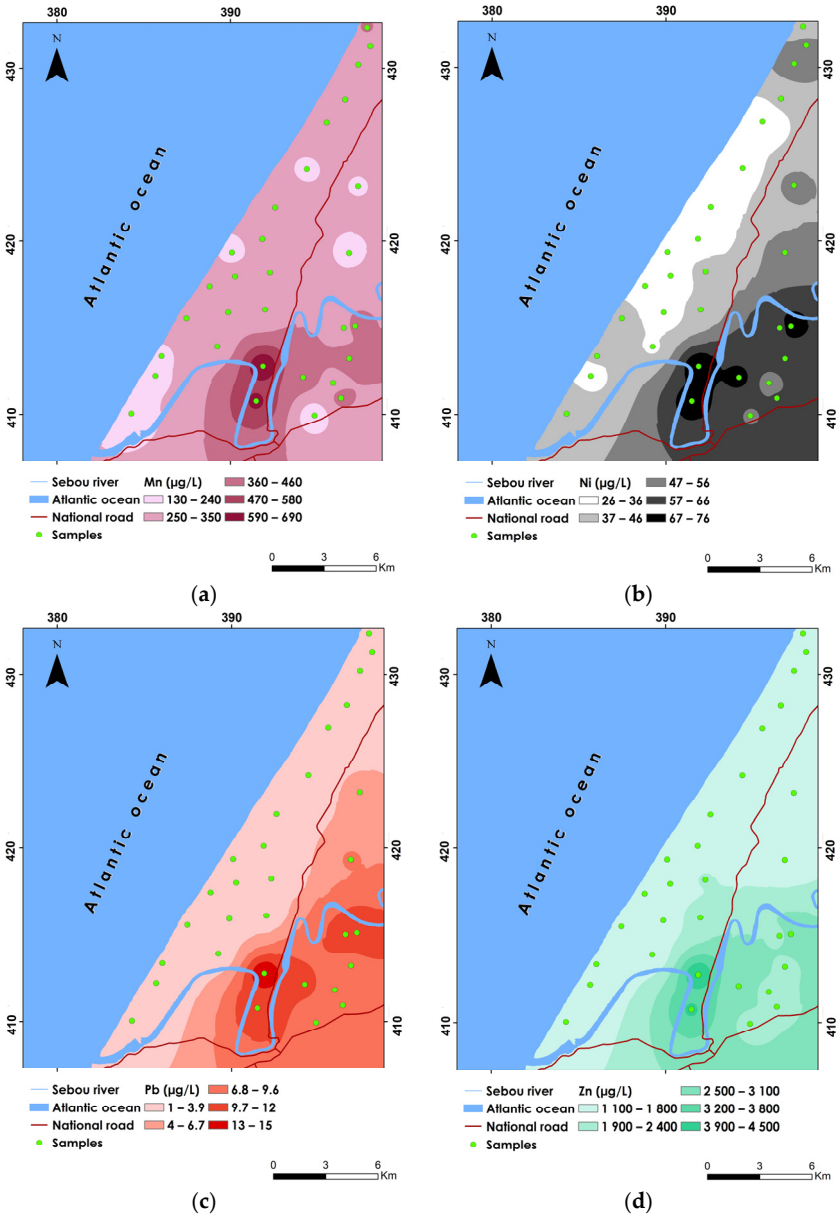


Figure 4. Spatial distribution maps of (**a**) Mn, (**b**) Ni, (**c**) Pb, and (**d**) Zn.

Lead (Pb) is notorious for its toxicity, known to enter living organisms through water, food, and inhalation, posing severe health risks [114]. The results indicate that Pb concentrations ranged from 1.03 to 15.25 µg/L, with a mean concentration of 4.43 µg/L and a standard deviation of 4.35 µg/L (Table 7). The CV% was 0.98, indicating considerable variability in Pb levels across the samples. Sample P29 exhibited the highest Pb concentration, while the lowest was observed in sample P13. The elevated Pb concentrations were predominantly found in the southern, southeastern, and eastern parts of the study area, ranging from 9.7 to 15 µg/L. In contrast, the central, western, and northern regions of the study area exhibited lower concentrations, with values recorded below 3.9 µg/L (Figure 4c). Approximately 16.66% of the samples (P4, P5, P6, P29, and P30) exceeded the WHO limit

of 10 µg/L. The elevated Pb levels in these areas likely stem from anthropogenic practices such as agricultural practices involving the use of lead-based pesticides or fertilizers, combustion of agricultural waste, landfill leachate, and disposal of waste [115]. These activities contribute to the introduction and accumulation of lead in groundwater, posing risks to both environmental and human health.

Zinc (Zn), crucial for enzyme function and various physiological processes, plays a vital role in human and animal nutrition [116]. The Zn concentrations ranged widely from 1057.50 to 4525.40 µg/L, with a mean concentration of 1727.51 µg/L and a standard deviation of 904.38 µg/L (Table 7). The coefficient of variation (CV%) was 0.52, indicating moderate variability in Zn levels across the sampled locations. Sample P29 recorded the highest Zn concentration, while the lowest was observed in sample P13. The spatial analysis shows that the elevated Zn concentrations were predominantly found in the southern, southeastern, and eastern parts of the study area, exceeding 2500 µg/L (Figure 4d). In contrast, the study site's northern, central, and western regions exhibited lower concentrations, with levels not exceeding 1800 µg/L. Approximately 6.66% of the samples (P29 and P30) exceeded the WHO limit of 3000 µg/L. The elevated Zn levels in these areas are likely attributable to agricultural practices involving the application of zinc-containing fertilizers and pesticides.

3.2. Multivariate Statistical Analysis

3.2.1. Correlation Matrix Analysis

Correlation analysis is a statistical technique employed in water quality research, offering valuable insights into how different variables interact and impact the chemical composition of water [117,118]. In this study, a Pearson correlation was constructed using the data from 10 chosen HM parameters, as detailed in Table 8.

Table 8. Pearson correlation matrix between HM concentrations.

	As	Cd	Cr	Cu	Fe	Hg	Mn	Ni	Pb	Zn
As	1									
Cd	−0.568	1								
Cr	−0.310	0.669	1							
Cu	0.532	−0.588	−0.451	1						
Fe	−0.308	0.761	0.613	0.720	1					
Hg	0.791	−0.496	0.717	0.596	−0.589	1				
Mn	0.429	−0.564	−0.482	0.460	0.511	0.428	1			
Ni	−0.585	0.895	0.701	−0.532	0.709	0.578	−0.446	1		
Pb	−0.215	0.646	0.747	−0.506	0.652	0.736	−0.449	0.672	1	
Zn	0.837	−0.651	−0.648	0.445	0.463	0.660	0.566	0.573	−0.796	1



The As exhibits significant strong positive correlations with Hg (r = 0.791) and Zn (r = 0.837), indicating that these metals may co-occur due to similar geochemical sources [119]. The positive correlation with Cu (r = 0.532) and Mn (r = 0.429) further supports the notion of combined natural and anthropogenic influences, such as industrial discharges or the weathering of mineral deposits [79]. The significant negative correlations with Cd, Cr, Fe, Ni, and Pb suggest different sources or pathways for these metals, possibly due to distinct industrial processes or agricultural practices [57]. The Cd demonstrates strong positive correlations with Cr (r = 0.669), Fe (r = 0.761), Ni (r = 0.701), and Pb (r = 0.646), implying that these metals might originate from the application of phosphate fertilizers [120]. The significant negative correlations with Cu, Hg, Mn, and Zn highlight the divergent sources or behaviors of these metals within the aquifer, possibly due to differences in their geochemical properties and interactions with the groundwater matrix [31].

The Cr shares strong positive correlations with Fe (r = 0.613), Hg (r = 0.717), Ni (r = 0.701), and Pb (r = 0.747), indicating potential common sources such as landfill effluents, and metal and waste disposal [115]. The negative correlations with Cu, Mn, and Zn suggest distinct geochemical processes or agricultural activities in the region. The Cu shows a strong positive correlation with Fe (r = 0.720), alongside significant positive correlations with Hg, Mn, and Zn, which may indicate shared anthropogenic sources such as agricultural runoff and fertilizers [121]. In contrast, it showed a negative correlation with Ni (r = −0.532) and Pb (r = −0.506). Fe is strongly positively correlated with Ni (r = 0.709) and Pb (r = 0.652), with positive correlations also observed with Mn and Zn. The positive correlations among Hg, Mn, Ni, and Zn further emphasize the interconnected nature of these metals, suggesting they often co-occur in groundwater due to similar sources or geochemical processes [122].

3.2.2. Principal Component Analysis

The PCA is an essential statistical method for examining complex datasets with numerous parameters and extensive data variations. Principal components (PCs) with high eigenvalues were considered to capture the most significant variations among different HM parameters [68].

The PCA for ten variables facilitated the extraction of two PCs, which collectively account for 76.70% of the total variance observed in the dataset (Table 9). Notably, the PC1-PC2 combination accounts for over 76.71% of the dataset's variability (Figure 5), suggesting that the HM variation of groundwater is predominantly captured within these two components.

PC1 captures 66.47% of the total variance, showing strong positive associations with As, Cu, Hg, Mn, and Zn (loading values > 0.750). The strong positive loadings of these metals imply that they are highly correlated and may originate from related anthropogenic activities, such as the use of chemical fertilizers, pesticides, and industrial processes prevalent in the south and southeast parts of the study area. These regions, characterized by extensive agricultural practices and the presence of uncontrolled landfills, contribute to the leaching of these metals into the groundwater. For instance, the overuse of chemical fertilizers and manure can introduce Cu and Zn into the soil, which subsequently leach into the groundwater [5]. Similarly, industrial activities and improper waste disposal can release Hg and As into the environment, further contaminating the groundwater [123]. Meanwhile, PC2, which accounts for 10.23% of the total variance, is characterized by high positive loadings of Cd, Cr, Fe, Ni, and Pb. The high positive loadings on PC2 indicate that these metals are likely influenced by geogenic factors, such as the natural composition of the earth's crust, and by specific anthropogenic activities, including industrial emissions and phosphorus fertilizers [103,124].

Table 9. Principal component analysis results of selected HM parameters.

Parameters	Components	
	PC1	**PC2**
As	0.879	−0.378
Cd	−0.361	0.840
Cr	−0.246	0.873
Cu	0.705	−0.386
Fe	−0.401	0.811
Hg	0.814	−0.230
Mn	0.638	−0.233
Ni	−0.272	0.826
Pb	−0.266	0.885
Zn	0.848	−0.358
Eigenvalue	6.648	1.023
Variability (%)	66.475	10.232
Cumulative (%)	66.475	76.707

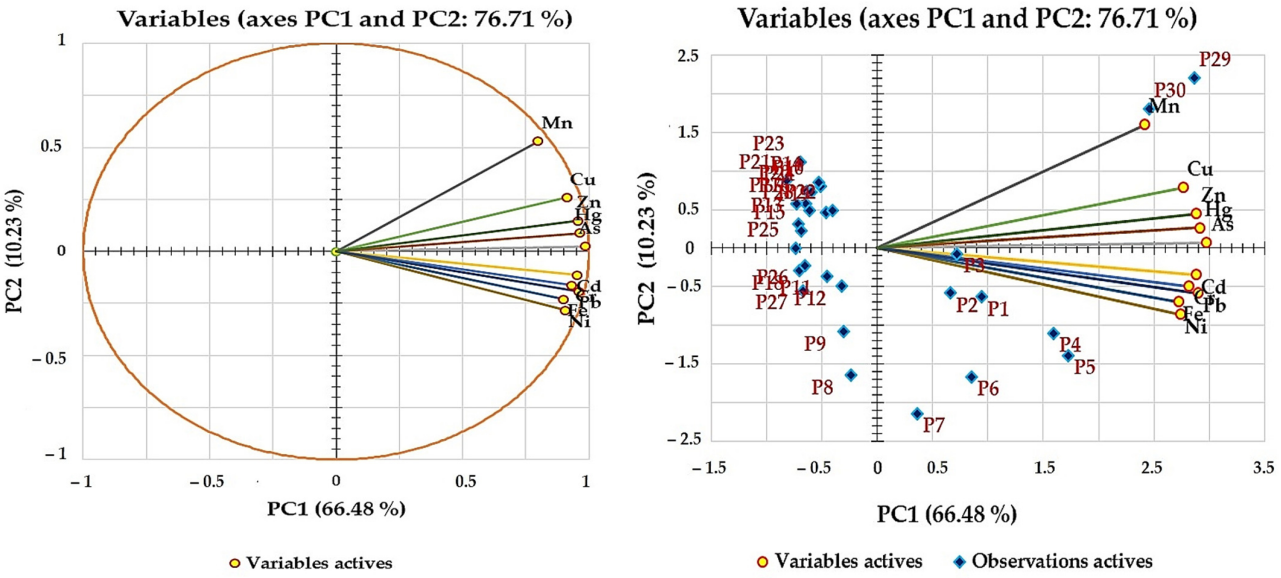


Figure 5. Principal component analysis for groundwater analysis.

3.2.3. Hierarchical Cluster Analysis

As part of our research, HCA was performed using the Ward linkage method in conjunction with Euclidean distance metrics [125]. This approach effectively grouped the heavy metals (HMs) into three distinct clusters, each reflecting specific similarities in their distribution and behavior (Figure 6).

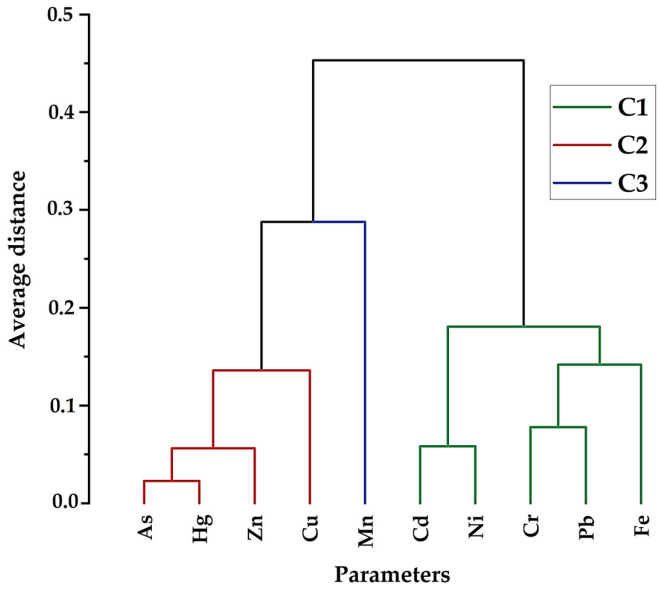


Figure 6. Dendrogram of the selected HMs.

The C1 cluster is segmented into two distinct sub-clusters. The first sub-cluster includes Cd and Ni. Both Cd and Ni are known to originate from industrial activities and agricultural practices [112]. The second sub-cluster within C1 comprises Cr-Pb, which is further linked to Fe. The linkage with Fe indicates that these metals may also be influenced by geogenic factors, given that Fe is prevalent in the earth's crust and can be mobilized through weathering processes.

The C2 contains a group of As-Hg, which are linked to Zn, and further connected to Cu. The release of both As and Hg is often attributed to farming practices, particularly through the application of arsenic-based pesticides and fungicides containing mercury [30]. Zn and

Cu, which are essential nutrients but can become contaminants at higher concentrations, are often introduced into the environment through the application of fertilizers and industrial activities [102]. The linkage of Zn and Cu with As and Hg indicates that these metals might be co-mobilized through agricultural runoff, industrial discharges, and landfill leachate [54].

The C3 is characterized by the presence of Mn, which is further linked to C2. The Mn is primarily derived from the suspension of manganese oxides and manganese-containing carbonate minerals in groundwater, with additional contributions from agricultural activities involving fertilizers and pesticides [126].

3.3. Pollution Assessment Using HMs Pollution Indices

3.3.1. Heavy Metal Pollution Index (HPI)

In the agricultural ecosystem under study, the HPI values ranged from 20.23 to 128.60, with a mean of 48.42 (Table 10). These values highlight varying degrees of groundwater contamination across different regions within the study area.

Table 10. Water quality classifications according to HPI, MI, C_d, and ERI values.

Samples	HPI Value	Class	MI Value	Class	C_d Value	Class	ERI Value	Class
P1	76.24	High water pollution	7.39	Seriously affected	6.95	High	52.48	Low ecological risk
P2	69.97	High water pollution	6.65	Seriously affected	6.21	High	49.18	Low ecological risk
P3	69.70	High water pollution	6.93	Seriously affected	6.49	High	48.84	Low ecological risk
P4	100.02	High water pollution	8.91	Seriously affected	8.47	High	67.09	Low ecological risk
P5	100.32	High water pollution	9.27	Seriously affected	8.83	High	66.89	Low ecological risk
P6	70.85	High water pollution	7.23	Seriously affected	6.79	High	48.95	Low ecological risk
P7	63.49	High water pollution	5.88	Strongly affected	5.44	High	44.67	Low ecological risk
P8	37.93	High water pollution	4.75	Strongly affected	4.31	High	26.37	Low ecological risk
P9	48.36	High water pollution	4.24	Strongly affected	3.80	High	34.61	Low ecological risk
P10	28.62	Medium water pollution	3.91	Moderately affected	3.47	High	22.69	Low ecological risk
P11	32.06	High water pollution	3.92	Moderately affected	3.48	High	25.31	Low ecological risk
P12	42.60	High water pollution	4.12	Strongly affected	3.68	High	32.51	Low ecological risk
P13	24.43	Medium water pollution	3.44	Moderately affected	3.00	High	19.93	Low ecological risk
P14	29.73	Medium water pollution	3.88	Moderately affected	3.44	High	23.08	Low ecological risk
P15	24.08	Medium water pollution	3.63	Moderately affected	3.19	High	18.79	Low ecological risk
P16	25.74	Medium water pollution	3.70	Moderately affected	3.26	High	19.85	Low ecological risk
P17	22.74	Medium water pollution	3.53	Moderately affected	3.09	High	18.31	Low ecological risk
P18	24.93	Medium water pollution	3.52	Moderately affected	3.08	High	19.32	Low ecological risk
P19	27.80	Medium water pollution	4.19	Strongly affected	3.74	High	21.53	Low ecological risk
P20	22.08	Medium water pollution	3.78	Moderately affected	3.34	High	17.69	Low ecological risk
P21	22.72	Medium water pollution	3.34	Moderately affected	2.90	Medium	17.30	Low ecological risk
P22	36.56	High water pollution	4.35	Strongly affected	3.91	High	26.61	Low ecological risk
P23	20.23	Medium water pollution	3.62	Moderately affected	3.18	High	16.91	Low ecological risk
P24	29.00	Medium water pollution	3.62	Moderately affected	3.18	High	23.68	Low ecological risk
P25	25.65	Medium water pollution	3.44	Moderately affected	3.00	High	20.09	Low ecological risk
P26	26.16	Medium water pollution	3.54	Moderately affected	3.10	High	20.82	Low ecological risk
P27	28.74	Medium water pollution	3.42	Moderately affected	2.98	Medium	23.48	Low ecological risk
P28	23.66	Medium water pollution	3.70	Moderately affected	3.26	High	19.79	Low ecological risk
P29	128.60	High water pollution	12.17	Seriously affected	1173	High	88.28	Low ecological risk
P30	117.74	High water pollution	11.11	Seriously affected	10.67	High	81.57	Low ecological risk

The groundwater quality, as categorized by the HPI, falls into two main classes: "Medium water pollution" and "High water pollution". Specifically, 53.33% of the samples fall within the "Medium water pollution" category, indicating moderate contamination levels with HPI values ranging between 15 and 30. This suggests that while the water in these areas is affected by heavy metal contamination, it is not at critically high levels. The moderate pollution levels could be attributed to both natural processes, such as the leaching of minerals from the soil, and anthropogenic activities, including agricultural runoff and the use of fertilizers. On the other hand, 46.66% of the samples are classified under "High water pollution", with HPI values exceeding 30. This significant proportion indicates a severe contamination issue in nearly half of the samples analyzed. The highest HPI values were recorded at sample locations P29 (128.60) and P30 (117.74), pointing to extremely high

levels of heavy metal pollution in these areas. The spatial distribution of HPI values shows that the highest pollution levels are indicated in the south and southeast parts of the study site (Figure 7a). This geographic trend correlates with the areas characterized by extensive agricultural activities, overuse of chemical fertilizers, and the presence of uncontrolled landfills. Conversely, the lowest HPI values were found in the north, central, and western parts of the study area, with the lowest recorded at sample P23.

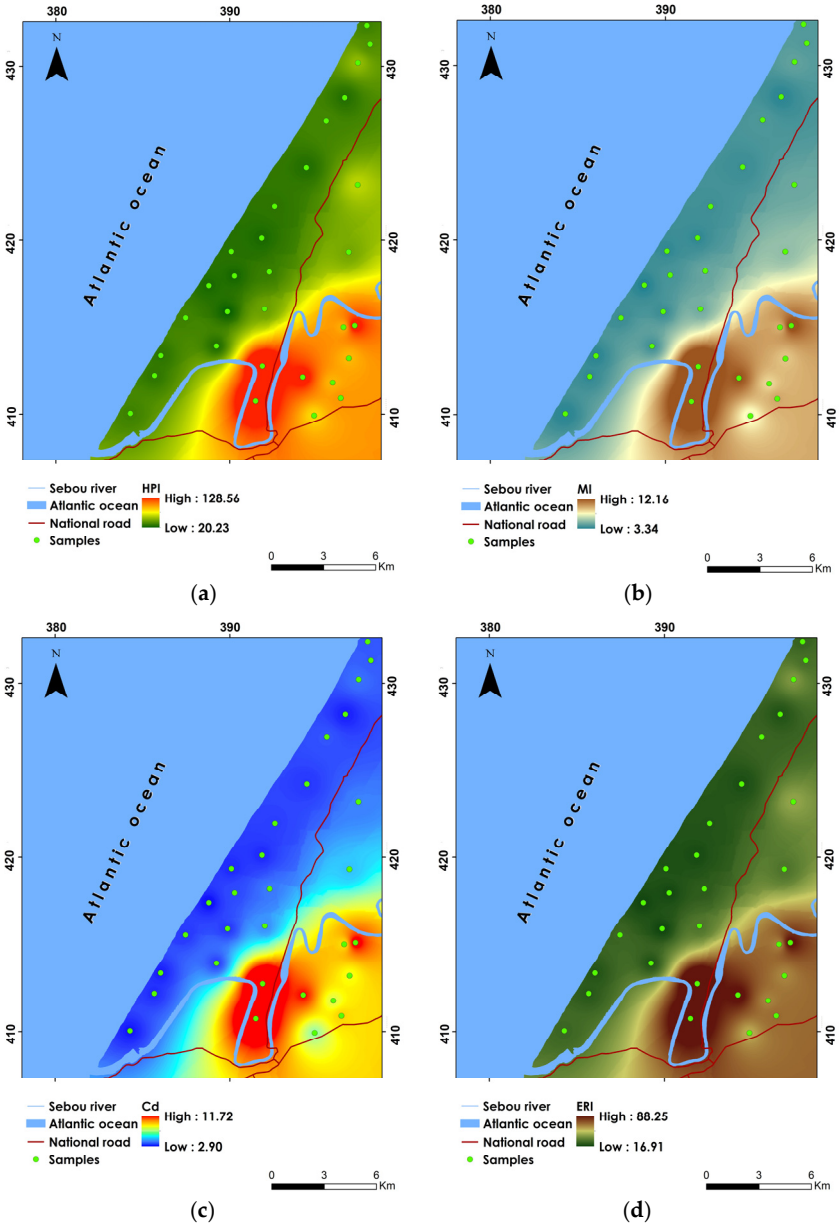


Figure 7. Spatial distribution maps of (**a**) HPI, (**b**) MI, (**c**) C_d, and (**d**) ERI.

3.3.2. Metal Index (MI)

The MI values ranged from 3.34 to 12.17, with an average value of 5.33 (Table 10). According to MI, groundwater is classified into three distinct classes: "Moderately affected", "Strongly affected", and "Seriously affected". Notably, 53.33% of the samples fall within the "Moderately affected" category, with MI values ranging between 2 and 4. This indicates that over half of the groundwater samples exhibit moderate levels of heavy metal contamination. Such levels, while not immediately hazardous, suggest a need for ongoing monitoring and potential remediation to prevent further degradation [79]. Conversely, 20% of the samples are classified as "Strongly affected", with MI values between 4 and 6. This

category reflects a significant increase in contamination levels, likely due to both natural and anthropogenic sources such as the extensive use of chemical fertilizers, industrial activities, and improper waste management practices [41]. Most concerning is the "Seriously affected" category, which includes 26.66% of the samples with MI values exceeding 6. This category underscores severe contamination issues, particularly in sample P29, which recorded the highest MI value of 12.17. The spatial analysis of MI values indicates that the highest levels of contamination are concentrated in the south and eastern parts of the study site (Figure 7b). The minimum MI values were recorded in the northern, central, and western regions of the study area, with sample P21 showing the lowest value. These areas appear to be less impacted by heavy metal contamination, potentially due to more sustainable agricultural practices.

3.3.3. Degree of Contamination (C_d)

The study reveals that C_d concentrations range from 2.90 to 11.73, with an average of 4.89, highlighting considerable variability in contamination levels throughout the study region (Table 10). Notably, only 6.66% of the samples fall within the "Medium" contamination category, with C_d values between 1 and 3. This minor subset, represented by samples P21 and P27, suggests that these locations have relatively lower contamination levels compared to the rest of the study area. Conversely, a substantial 93.33% of the samples are classified under "High" contamination ($C_d > 3$). The highest C_d is observed in sample P29, with a C_d value of 11.73, underscoring severe pollution issues likely resulting from intensive anthropogenic activities such as the use of chemical fertilizers, industrial discharges, and inadequate waste management. The spatial distribution of C_d values reveals that the highest contamination levels are concentrated in the south and eastern parts of the study area (Figure 7c). Conversely, the lowest C_d concentrations were identified in the northern, central, and western parts of the site. These areas appear to be less affected by heavy metal contamination, potentially due to more effective pollution control measures or less intensive agricultural and industrial activities.

3.3.4. Ecological Risk Index (ERI)

The ERI is a critical metric used to assess the potential ecological risk posed by heavy metals in groundwater [28]. The ERI values range from 16.91 to 88.28, with an average of 35.06 (Table 10). Furthermore, all groundwater samples in the study area were classified under the "Low ecological risk" category, as the ERI values remained below 150. This classification indicates that, despite the presence of heavy metals, the overall ecological risk to the environment remains low. Such a finding is somewhat reassuring, as it implies that the current levels of heavy metals are not likely to cause significant adverse effects on the local ecosystem in the short term. However, the spatial distribution of ERI values reveals that the highest risks are concentrated in the south and southeast parts of the study area (Figure 7d). Sample P29, with the highest ERI value of 88.28, highlights a zone where the cumulative presence of heavy metals is more pronounced. In contrast, the lowest ERI values are observed in the north, central, and western parts of the study area, with the lowest value recorded in sample P23.

3.3.5. Pollution Index (PI)

The PI is a crucial parameter used to assess the extent of heavy metal contamination in groundwater, providing insights into potential environmental and health impacts [45]. The calculated PI values range from 0.53 to 1.22, indicating varying levels of pollution among the different heavy metals (Table 11).

The analysis shows that most heavy metals, including As, Cd, Cr, Cu, Hg, Ni, Pb, and Zn, fall under the "No effect" category with PI values below 1. This suggests that, for these metals, groundwater contamination is relatively low and not likely to cause significant adverse effects on human health or the environment under current conditions. For instance, Hg has the lowest PI value, indicating minimal contamination and thus

posing the least risk among the evaluated heavy metals. However, Fe and Mn have PI values between 1 and 2, placing them in the "Slightly affected" category. This indicates a moderate level of contamination for these metals, which could potentially affect water quality. The Fe with the highest PI value suggests that its concentration in the groundwater is particularly concerning.

Table 11. Classification of selected HMs according to PI.

Parameters	As	Cd	Cr	Cu	Fe	Hg	Mn	Ni	Pb	Zn
PI values	0.58	0.83	0.69	0.61	1.22	0.53	1.14	0.58	0.94	0.93
Effect	No effect	No effect	No effect	No effect	Slightly affected	No effect	Slightly affected	No effect	No effect	No effect

3.4. Human Health Risk Assessment (HHRA)

The non-carcinogenic risk assessment provides crucial insights into the potential health hazards posed by HMs in groundwater. By evaluating the HQ and HI for both adults and children through ingestion and dermal exposure routes, the health risks have been calculated based on various toxic elements, including As, Cd, Cr, Cu, Fe, Hg, Mn, Ni, Pb, and Zn (Table 12).

Table 12. Evaluation of the potential health risks posed by HMs.

Parameters	R_fD		CDI_i		CDI_d		HQ_i		HQ_d		HI	
	R_fD_i	R_fD_d	Adult	Children	Adult	Children	Adult	Children	Adult	Children	Adult	Children
As	0.3	0.123	0.0860	0.0963	0.0004	0.0006	0.2866	0.3210	0.0035	0.0045	0.2901	0.3255
Cd	0.5	0.005	0.0531	0.0595	0.0003	0.0003	0.1063	0.1190	0.0536	0.0687	0.1599	0.1878
Cr	3	0.015	0.8288	0.9282	0.0084	0.0107	0.2763	0.3094	0.5569	0.7147	0.8332	1.0241
Cu	40	12	15.7092	17.5943	0.0792	0.1016	0.3927	0.4399	0.0066	0.0085	0.3993	0.4483
Fe	300	45	11.1976	12.5413	0.0564	0.0724	0.0373	0.0418	0.0013	0.0016	0.0386	0.0434
Hg	0.3	0.3	0.0386	0.0432	0.0002	0.0002	0.1286	0.1440	0.0006	0.0008	0.1292	0.1448
Mn	24	0.96	8.7073	9.7522	0.0439	0.0563	0.3628	0.4063	0.0457	0.0587	0.4085	0.4650
Ni	20	0.8	1.2852	1.4394	0.0065	0.0083	0.0643	0.0720	0.0081	0.0104	0.0724	0.0824
Pb	1.4	0.42	0.1266	0.1418	0.0006	0.0008	0.0905	0.1013	0.0015	0.0020	0.0920	0.1033
Zn	300	60	49.3576	55.2805	0.2488	0.3192	0.1645	0.1843	0.0041	0.0053	0.1687	0.1896

The HQ values for ingestion indicate that the non-carcinogenic risk varies significantly among the different HMs. For adults, HQi ranges from 0.0373 for Fe to 0.3927 for Cu. For children, these values range from 0.0418 for Fe to 0.4399 for Cu, indicating that children are more susceptible to heavy metal exposure than adults. This increased susceptibility is reflected in the higher mean HQi for children (0.21) compared to adults (0.19). Similarly, the HQ values for dermal exposure highlight varying levels of risk. For adults, HQd ranges from 0.0006 for Hg to 0.5569 for Cr, while for children, it ranges from 0.0008 for Hg to 0.7147 for Cr. Again, children exhibit higher mean HQd values (0.08) compared to adults (0.06), underscoring their greater vulnerability to dermal exposure to heavy metals. The HI, which aggregates the risk from all HMs, provides a broader view of the potential health impact. For adults, the HI values range from 0.0724 for Ni to 0.8332 for Cr. For children, the HI ranges from 0.0434 for Hg to 1.0241 for Cr. Notably, all HMs except for Cr have HI values less than 1 for both adults and children, indicating a low overall health risk from these metals. However, chromium stands out with an HI value greater than 1 for children, signifying a significant health risk.

The TCR assessment provides critical insights into the potential health risks associated with exposure to carcinogenic heavy metals (As, Cd, Cr, Ni, and Pb) in groundwater. The carcinogenic risk was evaluated separately for adults and children, considering both ingestion and dermal exposure routes, as outlined in (Table 13).

Table 13. Carcinogenic risk of various HMs in groundwater.

Parameters	CR_i		CR_d		TCR	
	Adult	Children	Adult	Children	Adult	Children
As	1.3×10^{-4}	1.4×10^{-4}	6.5×10^{-7}	8.34×10^{-7}	1.3×10^{-4}	1.5×10^{-4}
Cd	8×10^{-4}	8.9×10^{-4}	4.01×10^{-6}	5.15×10^{-6}	8×10^{-4}	9×10^{-4}
Cr	4.1×10^{-4}	4.6×10^{-4}	4.17×10^{-6}	5.36×10^{-6}	4.2×10^{-4}	4.7×10^{-4}
Ni	2.18×10^{-3}	2.45×10^{-3}	1.1×10^{-5}	1.41×10^{-5}	2.2×10^{-3}	2.46×10^{-3}
Pb	2.2×10^{-4}	2.4×10^{-4}	1.08×10^{-6}	1.39×10^{-6}	2.2×10^{-4}	2.4×10^{-4}

For adults, the TCR values for individual metals are as follows: As (1.3×10^{-4}), Cd (8×10^{-4}), Cr (4.2×10^{-4}), Ni (2.2×10^{-3}), and Pb (2.2×10^{-4}). The mean TCR for adults is 7.5×10^{-4}, suggesting that the cumulative carcinogenic risk from these metals is significantly above the negligible risk threshold of 10^{-6}. The TCR values for each metal fall within the range of acceptable or tolerable risk (10^{-6} to 10^{-4}) for As, Cr, and Pb, but Cd and Ni exceed this range, indicating a high risk and potential health detriments. Nickel, with the highest TCR of 2.2×10^{-3}, poses the greatest carcinogenic risk to adults among the metals analyzed. Children exhibit higher TCR values compared to adults for all the metals considered: As (1.5×10^{-4}), Cd (9×10^{-4}), Cr (4.7×10^{-4}), Ni (2.46×10^{-3}), and Pb (2.4×10^{-4}). The mean TCR for children is 8.4×10^{-4}, indicating a heightened carcinogenic risk relative to adults. Similar to adults, the TCR for As, Cr, and Pb falls within the acceptable or tolerable risk range, whereas Cd and Ni again show values that surpass the acceptable limits, suggesting a high risk. Nickel, with a TCR of 2.46×10^{-3}, remains the most significant contributor to carcinogenic risk in children. The TCR values indicate that both adults and children in the study area are exposed to carcinogenic risks that are notably above the negligible threshold. The higher susceptibility of children to these risks is particularly concerning, given their developing bodies and longer future exposure duration.

4. Conclusions

Groundwater, a primary source of freshwater, is experiencing quality degradation globally due to intensified anthropogenic activities, particularly industrialization and agricultural practices. This research investigates groundwater contamination by HMs within an agricultural ecosystem, focusing on water used for drinking and irrigation. To accomplish the research objectives, a total of thirty groundwater samples were systematically collected from different locations within the study area. These samples were analyzed using a combination of GIS methodology, statistical techniques, various pollution indices, and HHRA.

The results indicated notable variations in the concentrations of HMs in the study region, with the highest concentrations found in the southern and southeastern parts, areas characterized by intense agricultural and industrial activities and the presence of uncontrolled landfills. Statistical analyses, including PCA and HCA, identified significant correlations and clustering of metals, suggesting both natural and anthropogenic sources of contamination. Pollution indices revealed medium to high water pollution levels, with most samples indicating high contamination. HPI values ranged from 20.23 to 128.60, categorizing water pollution levels from medium to high, with 46.66% of samples classified as "High water pollution". MI values ranged from 3.34 to 12.17, indicating water quality ranging from moderately to seriously affected, with 53.33% of samples in the "Moderately affected" category, 20% as "Strongly affected", and 26.66% as "Seriously affected". The C_d values ranged from 2.90 to 11.73, with 93.33% of samples classified as "High". Although ERI values indicated a low ecological risk across all samples, health risk assessments highlighted significant non-carcinogenic and carcinogenic risks, particularly for children. TCR values for heavy metals such as Ni and Cr exceeded safe limits, indicating potential health hazards.

This research offers an in-depth analysis of the existing groundwater contamination levels by heavy metals, underscoring the associated health and environmental hazards. The insights provided by this study are crucial for policymakers and relevant stakeholders in devising strategies for effective groundwater management and pollution mitigation. The findings emphasize the necessity for stringent regulations on chemical fertilizer use and industrial discharges, improved waste management practices, and sustainable agricultural practices to mitigate heavy metal leaching into groundwater. Future research should focus on longitudinal monitoring of groundwater quality, expanding the scope to include additional contaminants, and developing advanced remediation techniques to reduce heavy metal concentrations in groundwater.

Author Contributions: Conceptualization, H.S. and M.O.L.; methodology, H.S., M.O.L. and A.Z.; software, H.S.; Resources, H.S. and M.O.L.; validation, H.S., L.M., A.Z. and H.D.; formal analysis, H.S., L.M., A.Z., R.M. and H.D.; writing—original draft preparation, H.S., A.Z., M.O.L. and L.M.; writing—review and editing, H.S., H.D., A.Z., R.M., M.O.L. and L.M.; visualization, H.S. and M.O.L.; supervision, A.Z., H.D. and L.M.; funding acquisition, R.M. All authors have read and agreed to the published version of the manuscript.

Funding: This research received no external funding.

Data Availability Statement: The authors strongly encourage interested researchers to contact us as we are more than willing to share the data upon request.

Acknowledgments: The authors would like to thank all those who collaborated in this work with the field sampling, laboratory analysis, and writing manuscript teams from the Laboratory of Process Engineering and Environment, National Institute of Agricultural Research (INRA), and International Center for Agricultural Research in the Dry Areas (ICARDA) in Morocco. The authors would like to thank the "MCGP" and "Climber" projects for their financial support.

Conflicts of Interest: The authors declare no conflicts of interest.

References

1. Wu, F.; Yang, X.; Cui, Z.; Ren, L.; Jiang, S.; Liu, Y.; Yuan, S. The Impact of Human Activities on Blue-Green Water Resources and Quantification of Water Resource Scarcity in the Yangtze River Basin. *Sci. Total Environ.* **2024**, *909*, 168550. [CrossRef]
2. Andrabi, S.; Bakhtiyar, Y.; Yousuf, T.; Akhtar, M.; Nissar, S. Water Quality Assessment in Relation to Fish Assemblage Using Multivariate Analysis in Manasbal Lake, Kashmir. *Water Sci.* **2024**, *38*, 92–108. [CrossRef]
3. Scanlon, B.R.; Fakhreddine, S.; Rateb, A.; de Graaf, I.; Famiglietti, J.; Gleeson, T.; Grafton, R.Q.; Jobbagy, E.; Kebede, S.; Kolusu, S.R.; et al. Global Water Resources and the Role of Groundwater in a Resilient Water Future. *Nat. Rev. Earth Environ.* **2023**, *4*, 87–101. [CrossRef]
4. Saleh, H.N.; Panahande, M.; Yousefi, M.; Asghari, F.B.; Oliveri Conti, G.; Talaee, E.; Mohammadi, A.A. Carcinogenic and Non-Carcinogenic Risk Assessment of Heavy Metals in Groundwater Wells in Neyshabur Plain, Iran. *Biol. Trace Elem. Res.* **2019**, *190*, 251–261. [CrossRef] [PubMed]
5. Abanyie, S.K.; Apea, O.B.; Abagale, S.A.; Amuah, E.E.Y.; Sunkari, E.D. Sources and Factors Influencing Groundwater Quality and Associated Health Implications: A Review. *Emerg. Contam.* **2023**, *9*, 100207. [CrossRef]
6. Wang, Y.; Yuan, X.; Zhang, Y.; Zhang, X.; Xiao, Y.; Duo, J.; Huang, X.; Sun, M.; Lv, G. Hydrochemical, D–O–Sr Isotopic and Electromagnetic Characteristics of Geothermal Waters from the Erdaoqiao Area, SW China: Insights into Genetic Mechanism and Scaling Potential. *Ore Geol. Rev.* **2023**, *158*, 105486. [CrossRef]
7. Gao, Y.; Qian, H.; Zhou, Y.; Chen, J.; Wang, H.; Ren, W.; Qu, W. Cumulative Health Risk Assessment of Multiple Chemicals in Groundwater Based on Deterministic and Monte Carlo Models in a Large Semiarid Basin. *J. Clean. Prod.* **2022**, *352*, 131567. [CrossRef]
8. Islam, M.S. Groundwater: Sources, Functions, and Quality. In *Hydrogeochemical Evaluation and Groundwater Quality*; Springer Nature: Cham, Switzerland, 2023; pp. 17–36, ISBN 978-3-031-44304-6.
9. Sharma, K.; Rajan, S.; Nayak, S.K. Chapter 1—Water Pollution: Primary Sources and Associated Human Health Hazards with Special Emphasis on Rural Areas. *Water Resour. Manag. Rural. Dev.* **2024**, *35*, 3–14.
10. Maharjan, A.K.; Kamei, T.; Amatya, I.M.; Mori, K.; Kazama, F.; Toyama, T. Ammonium-Nitrogen (NH_4^+-N) Removal from Groundwater by a Dropping Nitrification Reactor: Characterization of NH_4^+-N Transformation and Bacterial Community in the Reactor. *Water* **2020**, *12*, 599. [CrossRef]
11. Nurtazin, S.; Pueppke, S.; Ospan, T.; Mukhitdinov, A.; Elebessov, T. Quality of Drinking Water in the Balkhash District of Kazakhstan's Almaty Region. *Water* **2020**, *12*, 392. [CrossRef]

12. Rao, K.N.; Latha, P.S. Groundwater Quality Assessment Using Water Quality Index with a Special Focus on Vulnerable Tribal Region of Eastern Ghats Hard Rock Terrain, Southern India. *Arab. J. Geosci.* **2019**, *12*, 267. [CrossRef]
13. Kana, A.A. Heavy Metal Assessment of Groundwater Quality in Part of Karu, Central Nigeria. *Water Pract. Technol.* **2022**, *17*, 1802–1817. [CrossRef]
14. Feng, B.; Ma, Y.; Qi, Y.; Zhong, Y.; Sha, X. Health Risk Assessment of Groundwater Nitrogen Pollution in Yinchuan Plain. *J. Contam. Hydrol.* **2022**, *249*, 104031. [CrossRef] [PubMed]
15. Marghade, D. Detailed Geochemical Assessment & Indexing of Shallow Groundwater Resources in Metropolitan City of Nagpur (Western Maharashtra, India) with Potential Health Risk Assessment of Nitrate Enriched Groundwater for Sustainable Development. *Geochemistry* **2020**, *80*, 125627. [CrossRef]
16. Toi Bissang, B.; Aragón-Barroso, A.J.; Baba, G.; González-López, J.; Osorio, F. Integrated Assessment of Heavy Metal Pollution and Human Health Risks in Waters from a Former Iron Mining Site: A Case Study of the Canton of Bangeli, Togo. *Water* **2024**, *16*, 471. [CrossRef]
17. Saddik, M.; Fadili, A.; Makan, A. Assessment of Heavy Metal Contamination in Surface Sediments along the Mediterranean Coast of Morocco. *Environ. Monit. Assess.* **2019**, *191*, 197. [CrossRef]
18. Belkhiri, L.; Mouni, L.; Narany, T.S.; Tiri, A. Evaluation of Potential Health Risk of Heavy Metals in Groundwater Using the Integration of Indicator Kriging and Multivariate Statistical Methods. *Groundw. Sustain. Dev.* **2017**, *4*, 12–22. [CrossRef]
19. Khan, M.; Ellahi, A.; Niaz, R.; Ghoneim, M.E.; Tag-eldin, E.; Rashid, A. Water Quality Assessment of Alpine Glacial Blue Water Lakes and Glacial-Fed Rivers. *Geomat. Nat. Hazards Risk* **2022**, *13*, 2597–2617. [CrossRef]
20. Yin, X.; Shao, P.; Ding, L.; Xi, Y.; Zhang, K.; Yang, L.; Shi, H.; Luo, X. Protonation of Rhodanine Polymers for Enhancing the Capture and Recovery of Ag+ from Highly Acidic Wastewater. *Environ. Sci. Nano* **2019**, *6*, 3307–3315. [CrossRef]
21. Ge, X.; Ma, Y.; Song, X.; Wang, G.; Zhang, H.; Zhang, Y.; Zhao, H. β-FeOOH Nanorods/Carbon Foam-Based Hierarchically Porous Monolith for Highly Effective Arsenic Removal. *ACS Appl. Mater. Interfaces* **2017**, *9*, 13480–13490. [CrossRef]
22. Aithani, D.; Kushawaha, J. Heavy Metals Contamination in Environment. In *Remediation of Heavy Metals*; John Wiley & Sons, Ltd.: Hoboken, NJ, USA, 2024; pp. 15–30. ISBN 978-1-119-85358-9.
23. Rashid, A.; Schutte, B.J.; Ulery, A.; Deyholos, M.K.; Sanogo, S.; Lehnhoff, E.A.; Beck, L. Heavy Metal Contamination in Agricultural Soil: Environmental Pollutants Affecting Crop Health. *Agronomy* **2023**, *13*, 1521. [CrossRef]
24. Lace, A.; Cleary, J. A Review of Microfluidic Detection Strategies for Heavy Metals in Water. *Chemosensors* **2021**, *9*, 60. [CrossRef]
25. Kou, B.; Yuan, Y.; Zhu, X.; Ke, Y.; Wang, H.; Yu, T.; Tan, W. Effect of Soil Organic Matter-Mediated Electron Transfer on Heavy Metal Remediation: Current Status and Perspectives. *Sci. Total Environ.* **2024**, *917*, 170451. [CrossRef]
26. Gao, J.; Han, H.; Gao, C.; Wang, Y.; Dong, B.; Xu, Z. Organic Amendments for in Situ Immobilization of Heavy Metals in Soil: A Review. *Chemosphere* **2023**, *335*, 139088. [CrossRef] [PubMed]
27. Yasin, M.U.; Haider, Z.; Munir, R.; Zulfiqar, U.; Rehman, M.; Javaid, M.H.; Ahmad, I.; Nana, C.; Saeed, M.S.; Ali, B.; et al. The Synergistic Potential of Biochar and Nanoparticles in Phytoremediation and Enhancing Cadmium Tolerance in Plants. *Chemosphere* **2024**, *354*, 141672. [CrossRef]
28. Edo, G.I.; Samuel, P.O.; Oloni, G.O.; Ezekiel, G.O.; Ikpekoro, V.O.; Obasohan, P.; Ongulu, J.; Otunuya, C.F.; Opiti, A.R.; Ajakaye, R.S.; et al. Environmental Persistence, Bioaccumulation, and Ecotoxicology of Heavy Metals. *Chem. Ecol.* **2024**, *40*, 322–349. [CrossRef]
29. Bețianu, C.; Cozma, P.; Gavrilescu, M. Human Health Hazards and Risks Generated by the Bioaccumulation of Lead from the Environment in the Food Chain. In *Lead Toxicity Mitigation: Sustainable Nexus Approaches*; Kumar, N., Jha, A.K., Eds.; Springer Nature: Cham, Switzerland, 2024; pp. 73–123. ISBN 978-3-031-46146-0.
30. Sable, H.; Singh, V.; Kumar, V.; Roy, A.; Pandit, S.; Kaur, K.; Rustagi, S.; Malik, S. Toxicological and Bioremediation Profiling of Nonessential Heavy Metals (Mercury, Chromium, Cadmium, Aluminium) and Their Impact on Human Health: A Review. *Toxicol. Anal. Clin.* **2024**, *36*, 205–234. [CrossRef]
31. Tyczyńska, M.; Gędek, M.; Brachet, A.; Stręk, W.; Flieger, J.; Teresiński, G.; Baj, J. Trace Elements in Alzheimer's Disease and Dementia: The Current State of Knowledge. *J. Clin. Med.* **2024**, *13*, 2381. [CrossRef] [PubMed]
32. Ceramella, J.; De Maio, A.C.; Basile, G.; Facente, A.; Scali, E.; Andreu, I.; Sinicropi, M.S.; Iacopetta, D.; Catalano, A. Phytochemicals Involved in Mitigating Silent Toxicity Induced by Heavy Metals. *Foods* **2024**, *13*, 978. [CrossRef]
33. Anchidin-Norocel, L.; Gutt, G.; Tătăranu, E.; Amariei, S. Electrochemical Sensors and Biosensors: Effective Tools for Detecting Heavy Metals in Water and Food with Possible Implications for Children's Health. *Int. J. Electrochem. Sci.* **2024**, *19*, 100643. [CrossRef]
34. Zhu, Y.; Yang, Q.; Wang, H.; Yang, J.; Zhang, X.; Li, Z.; Martín, J.D. A Hydrochemical and Isotopic Approach for Source Identification and Health Risk Assessment of Groundwater Arsenic Pollution in the Central Yinchuan Basin. *Environ. Res.* **2023**, *231*, 116153. [CrossRef] [PubMed]
35. Budi, H.S.; Opulencia, M.J.C.; Afra, A.; Abdelbasset, W.K.; Abdullaev, D.; Majdi, A.; Taherian, M.; Ekrami, H.A.; Mohammadi, M.J. Source, Toxicity and Carcinogenic Health Risk Assessment of Heavy Metals. *Rev. Environ. Health* **2022**, *39*, 77–90. [CrossRef] [PubMed]
36. Ray, S.; Vashishth, R. From Water to Plate: Reviewing the Bioaccumulation of Heavy Metals in Fish and Unraveling Human Health Risks in the Food Chain. *Emerg. Contam.* **2024**, *10*, 100358. [CrossRef]

37. Althomali, R.H.; Abbood, M.A.; Saleh, E.A.M.; Djuraeva, L.; Abdullaeva, B.S.; Habash, R.T.; Alhassan, M.S.; Alawady, A.H.R.; Alsaalamy, A.H.; Najafi, M.L. Exposure to Heavy Metals and Neurocognitive Function in Adults: A Systematic Review. *Environ. Sci. Eur.* **2024**, *36*, 18. [CrossRef]
38. Wu, Y.-S.; Osman, A.I.; Hosny, M.; Elgarahy, A.M.; Eltaweil, A.S.; Rooney, D.W.; Chen, Z.; Rahim, N.S.; Sekar, M.; Gopinath, S.C.B.; et al. The Toxicity of Mercury and Its Chemical Compounds: Molecular Mechanisms and Environmental and Human Health Implications: A Comprehensive Review. *ACS Omega* **2024**, *9*, 5100–5126. [CrossRef]
39. Howard, R.; Al-Mayhani, T.; Carr, A.; Leff, A.; Morrow, J.; Rossor, A. Toxic, Metabolic and Physical Insults to the Nervous System. In *Neurology*; John Wiley & Sons, Ltd.: Hoboken, NJ, USA, 2024; pp. 903–943, ISBN 978-1-119-71567-2.
40. Shukla, S.; Mbingwa, G.; Khanna, S.; Dalal, J.; Sankhyan, D.; Malik, A.; Badhwar, N. Environment and Health Hazards Due to Military Metal Pollution: A Review. *Environ. Nanotechnol. Monit. Manag.* **2023**, *20*, 100857. [CrossRef]
41. Witkowski, A.J.; Dąbrowska, D.; Wróbel, J. Groundwater Quality Assessment in the Area of the Zinc Smelter in Miasteczko Śląskie (Poland) Using Selected Metal Indices. *Water* **2024**, *16*, 279. [CrossRef]
42. Zainudin, A.M.; Zulkefli, S.N.; Looi, L.J.; Aris, A.Z.; Sefie, A.; Isa, N.M. Spatial and Temporal Evaluation of Groundwater Hydrochemistry in an Active Phreatic Zone of Developed Basin in Selangor, Malaysia. *Appl. Geochem.* **2023**, *154*, 105656. [CrossRef]
43. Singh, K.K.; Tewari, G.; Kumar, S.; Busa, R.; Chaturvedi, A.; Rathore, S.S.; Singh, R.K.; Gangwar, A. Understanding Urban Groundwater Pollution in the Upper Gangetic Alluvial Plains of Northern India with Multiple Industries and Their Impact on Drinking Water Quality and Associated Health Risks. *Groundw. Sustain. Dev.* **2023**, *21*, 100902. [CrossRef]
44. Sarhat, A.R.; Al-Obaidi, B.S. Contamination by Heavy Metals in the Sediments of Sirwan/Diyala River, Garmian Region. *IOP Conf. Ser. Earth Environ. Sci.* **2023**, *1158*, 022010. [CrossRef]
45. Gad, M.; Abou El-Safa, M.M.; Farouk, M.; Hussein, H.; Alnemari, A.M.; Elsayed, S.; Khalifa, M.M.; Moghanm, F.S.; Eid, E.M.; Saleh, A.H. Integration of Water Quality Indices and Multivariate Modeling for Assessing Surface Water Quality in Qaroun Lake, Egypt. *Water* **2021**, *13*, 2258. [CrossRef]
46. Mukherjee, I.; Singh, U.K.; Singh, R.P.; Anshumali; Kumari, D.; Jha, P.K.; Mehta, P. Characterization of Heavy Metal Pollution in an Anthropogenically and Geologically Influenced Semi-Arid Region of East India and Assessment of Ecological and Human Health Risks. *Sci. Total Environ.* **2020**, *705*, 135801. [CrossRef] [PubMed]
47. Chaturvedi, A.; Bhattacharjee, S.; Mondal, G.C.; Kumar, V.; Singh, P.K.; Singh, A.K. Exploring New Correlation between Hazard Index and Heavy Metal Pollution Index in Groundwater. *Ecol. Indic.* **2019**, *97*, 239–246. [CrossRef]
48. Sawut, R.; Kasim, N.; Maihemuti, B.; Hu, L.; Abliz, A.; Abdujappar, A.; Kurban, M. Pollution Characteristics and Health Risk Assessment of Heavy Metals in the Vegetable Bases of Northwest China. *Sci. Total Environ.* **2018**, *642*, 864–878. [CrossRef]
49. Patel, N.; Bhatt, D. Insights of Ground Water Quality Assessment Methods—A Review. *Mater. Today Proc.* **2024**. [CrossRef]
50. Kandel, K.; Sharma, C.M.; Rawat, B.; Paudyal, R.; Li, M.; Pandey, A.; Zhang, Q. Synthesis Analysis of Hydrogeochemistry of Nepal Himalayan Rivers: Perspective from Major Ions and Trace Elements. *Ecol. Indic.* **2024**, *163*, 112080. [CrossRef]
51. Ribeiro, P.G.; de Oliveira, C.; Guerra, M.B.B.; de Carvalho, T.S.; Martins, G.C.; Pereira, W.V.d.S.; Ramos, S.J.; Guilherme, L.R.G. Rare Earths as Emerging Trace Element Contaminants in the Soil. *Curr. Pollut. Rep.* **2024**, *10*, 443–458. [CrossRef]
52. Onyena, A.P.; Folorunso, O.M.; Nwanganga, N.; Udom, G.J.; Ekhator, O.C.; Frazzoli, C.; Ruggieri, F.; Bocca, B.; Orisakwe, O.E. Engaging One Health in Heavy Metal Pollution in Some Selected Nigerian Niger Delta Cities. A Systematic Review of Pervasiveness, Bioaccumulation and Subduing Environmental Health Challenges. *Biol. Trace Elem. Res.* **2024**, *202*, 1356–1389. [CrossRef]
53. Zhang, S.; Han, Y.; Peng, J.; Chen, Y.; Zhan, L.; Li, J. Human Health Risk Assessment for Contaminated Sites: A Retrospective Review. *Environ. Int.* **2023**, *171*, 107700. [CrossRef]
54. Li, P.; Karunanidhi, D.; Subramani, T.; Srinivasamoorthy, K. Sources and Consequences of Groundwater Contamination. *Arch. Environ. Contam. Toxicol.* **2021**, *80*, 1–10. [CrossRef]
55. Wang, X.; Liu, B.; He, S.; Yuan, H.; Ji, D.; Li, R.; Song, Y.; Xu, W.; Liu, B.; Xu, Y. Groundwater Environment and Health Risk Assessment in an In Situ Oil Shale Mining Area. *Water* **2024**, *16*, 185. [CrossRef]
56. Yu, Z.; Yao, R.; Huang, X.; Yan, Y. Health Risk Appraisal of Trace Elements in Groundwater in an Urban Area: A Case Study of Sichuan Basin, Southwest China. *Water* **2023**, *15*, 4286. [CrossRef]
57. Badeenezhad, A.; Soleimani, H.; Shahsavani, S.; Parseh, I.; Mohammadpour, A.; Azadbakht, O.; Javanmardi, P.; Faraji, H.; Babakrpur Nalosi, K. Comprehensive Health Risk Analysis of Heavy Metal Pollution Using Water Quality Indices and Monte Carlo Simulation in R Software. *Sci. Rep.* **2023**, *13*, 15817. [CrossRef] [PubMed]
58. Munene, E.N.; Hashim, N.O.; Ambusso, W.N. Human Health Risk Assessment of Heavy Metal Concentration in Surface Water of Sosian River, Eldoret Town, Uasin-Gishu County Kenya. *MethodsX* **2023**, *11*, 102298. [CrossRef]
59. Selvam, S.; Manimaran, G.; Sivasubramanian, P.; Balasubramanian, N.; Seshunarayana, T. GIS-Based Evaluation of Water Quality Index of Groundwater Resources around Tuticorin Coastal City, South India. *Environ. Earth Sci.* **2014**, *71*, 2847–2867. [CrossRef]
60. Nduka, J.K.; Kelle, H.I.; Umeh, T.C.; Okafor, P.C.; Iloka, G.C.; Okoyomon, E. Ecological and Health Risk Assessment of Radionuclides and Heavy Metals of Surface and Ground Water of Ishiagu–Ezillo Quarry Sites of Ebonyi, Southeast Nigeria. *J. Hazard. Mater. Adv.* **2023**, *10*, 100307. [CrossRef]
61. Dippong, T.; Mihali, C.; Avram, A. Evaluating Groundwater Metal and Arsenic Content in Piatra, North-West of Romania. *Water* **2024**, *16*, 539. [CrossRef]

62. Rashid, A.; Ayub, M.; Ullah, Z.; Ali, A.; Sardar, T.; Iqbal, J.; Gao, X.; Bundschuh, J.; Li, C.; Khattak, S.A.; et al. Groundwater Quality, Health Risk Assessment, and Source Distribution of Heavy Metals Contamination around Chromite Mines: Application of GIS, Sustainable Groundwater Management, Geostatistics, PCAMLR, and PMF Receptor Model. *Int. J. Environ. Res. Public Health* **2023**, *20*, 2113. [CrossRef] [PubMed]
63. Liu, Z.; Tao, S.; Sun, Z.; Chen, Y.; Xu, J. Determination of Heavy Metals and Health Risk Assessment in Tap Water from Wuhan, China, a City with Multiple Drinking Water Sources. *Water* **2023**, *15*, 3709. [CrossRef]
64. Egbueri, J.C. Groundwater Quality Assessment Using Pollution Index of Groundwater (PIG), Ecological Risk Index (ERI) and Hierarchical Cluster Analysis (HCA): A Case Study. *Groundw. Sustain. Dev.* **2020**, *10*, 100292. [CrossRef]
65. Sanad, H.; Moussadek, R.; Mouhir, L.; Oueld Lhaj, M.; Dakak, H.; El Azhari, H.; Yachou, H.; Ghanimi, A.; Zouahri, A. Assessment of Soil Spatial Variability in Agricultural Ecosystems Using Multivariate Analysis, Soil Quality Index (SQI), and Geostatistical Approach: A Case Study of the Mnasra Region, Gharb Plain, Morocco. *Agronomy* **2024**, *14*, 1112. [CrossRef]
66. El Azhari, H.; Cherif, E.K.; El Halimi, R.; Azzirgue, E.M.; Ou Larbi, Y.; Coren, F.; Salmoun, F. Predicting the Production and Depletion of Rare Earth Elements and Their Influence on Energy Sector Sustainability through the Utilization of Multilevel Linear Prediction Mixed-Effects Models with R Software. *Sustainability* **2024**, *16*, 1951. [CrossRef]
67. Azhari, H.E.; Cherif, E.K.; Sarti, O.; Azzirgue, E.M.; Dakak, H.; Yachou, H.; Esteves Da Silva, J.C.G.; Salmoun, F. Assessment of Surface Water Quality Using the Water Quality Index (IWQ), Multivariate Statistical Analysis (MSA) and Geographic Information System (GIS) in Oued Laou Mediterranean Watershed, Morocco. *Water* **2022**, *15*, 130. [CrossRef]
68. Sanad, H.; Mouhir, L.; Zouahri, A.; Moussadek, R.; El Azhari, H.; Yachou, H.; Ghanimi, A.; Oueld Lhaj, M.; Dakak, H. Assessment of Groundwater Quality Using the Pollution Index of Groundwater (PIG), Nitrate Pollution Index (NPI), Water Quality Index (WQI), Multivariate Statistical Analysis (MSA), and GIS Approaches: A Case Study of the Mnasra Region, Gharb Plain, Morocco. *Water* **2024**, *16*, 1263. [CrossRef]
69. Aabad, M.; Bouaziz, A.; Falisse, A.; Martin, J.F. Improving Yield and Water Use Efficiency of Sugarcane under Drip. *Rev. Marocaine Des Sci. Agron. Vétérinaires* **2016**, *5*, 32–40.
70. Mrabet, L.; Loukili, A.; Belghyti, D.; Attarassi, B. Impact of Leachates from the Landfill in the Kenitra City (Morocco) on the Water Resources. *Int. J. Appl. Environ. Sci.* **2019**, *14*, 541–553.
71. Chow, A.T.-S.; Ulus, Y.; Huang, G.; Kline, M.A.; Cheah, W.-Y. Challenges in Quantifying and Characterizing Dissolved Organic Carbon: Sampling, Isolation, Storage, and Analysis. *J. Environ. Qual.* **2022**, *51*, 837–871. [CrossRef]
72. Wang, H.; Wu, Z.; Chen, B.; He, M.; Hu, B. Chip-Based Array Magnetic Solid Phase Microextraction on-Line Coupled with Inductively Coupled Plasma Mass Spectrometry for the Determination of Trace Heavy Metals in Cells. *Analyst* **2015**, *140*, 5619–5626. [CrossRef]
73. Tao, S.; Zhang, X.; Xu, J.; Pan, G.; Gu, F. Anthropogenic Impacts on Isotopic and Geochemical Characteristics of Urban Streams: A Case Study in Wuhan, China. *Environ. Sci. Pollut. Res.* **2021**, *28*, 39186–39198. [CrossRef]
74. El-Zeiny, A.M.; Kafrawy, S.B.E.; Ahmed, M.H. Geomatics Based Approach for Assessing Qaroun Lake Pollution. *Egypt. J. Remote Sens. Space Sci.* **2019**, *22*, 279–296. [CrossRef]
75. Pan, Y.; She, D.; Ding, J.; Abulaiti, A.; Zhao, J.; Wang, Y.; Liu, R.; Wang, F.; Shan, J.; Xia, Y. Coping with Groundwater Pollution in High-Nitrate Leaching Areas: The Efficacy of Denitrification. *Environ. Res.* **2024**, *250*, 118484. [CrossRef] [PubMed]
76. Prasad, M.; Sunitha, V.; Reddy, Y.S.; Suvarna, B.; Reddy, B.M.; Reddy, M.R. Data on Water Quality Index Development for Groundwater Quality Assessment from Obulavaripalli Mandal, YSR District, A.P India. *Data Brief* **2019**, *24*, 103846. [CrossRef] [PubMed]
77. Sheng, D.; Meng, X.; Wen, X.; Wu, J.; Yu, H.; Wu, M. Contamination Characteristics, Source Identification, and Source-Specific Health Risks of Heavy Metal(Loid)s in Groundwater of an Arid Oasis Region in Northwest China. *Sci. Total Environ.* **2022**, *841*, 156733. [CrossRef]
78. WHO World Health Organization. *Guidelines for Drinking-Water Quality: Fourth Edition Incorporating First Addendum*; World Health Organization: Geneva, Switzerland, 2017; ISBN 978-92-4-154995-0.
79. Wagh, V.M.; Panaskar, D.B.; Mukate, S.V.; Gaikwad, S.K.; Muley, A.A.; Varade, A.M. Health Risk Assessment of Heavy Metal Contamination in Groundwater of Kadava River Basin, Nashik, India. *Model. Earth Syst. Environ.* **2018**, *4*, 969–980. [CrossRef]
80. Tamasi, G.; Cini, R. Heavy Metals in Drinking Waters from Mount Amiata (Tuscany, Italy). Possible Risks from Arsenic for Public Health in the Province of Siena. *Sci. Total Environ.* **2004**, *327*, 41–51. [CrossRef] [PubMed]
81. Alam, R.; Ahmed, Z.; Howladar, M.F. Evaluation of Heavy Metal Contamination in Water, Soil and Plant around the Open Landfill Site Mogla Bazar in Sylhet, Bangladesh. *Groundw. Sustain. Dev.* **2020**, *10*, 100311. [CrossRef]
82. Caeiro, S.; Costa, M.H.; Ramos, T.B.; Fernandes, F.; Silveira, N.; Coimbra, A.; Medeiros, G.; Painho, M. Assessing Heavy Metal Contamination in Sado Estuary Sediment: An Index Analysis Approach. *Ecol. Indic.* **2005**, *5*, 151–169. [CrossRef]
83. Edet, A.E.; Offiong, O.E. Evaluation of Water Quality Pollution Indices for Heavy Metal Contamination Monitoring. A Study Case from Akpabuyo-Odukpani Area, Lower Cross River Basin (Southeastern Nigeria). *GeoJournal* **2002**, *57*, 295–304. [CrossRef]
84. Economou-Eliopoulos, M.; Megremi, I. Contamination of the Soil–Groundwater–Crop System: Environmental Risk and Opportunities. *Minerals* **2021**, *11*, 775. [CrossRef]
85. Botle, A.; Salgaonkar, S.; Tiwari, R.; Ambadekar, S.; Barabde, G.R. Brief Status of Contamination in Surface Water of Rivers of India by Heavy Metals: A Review with Pollution Indices and Health Risk Assessment. *Environ. Geochem. Health* **2023**, *45*, 2779–2801. [CrossRef]

86. Sudharshan Reddy, Y.; Sunitha, V. Assessment of Heavy Metal Pollution and Its Health Implications in Groundwater for Drinking Purpose around Inactive Mines, SW Region of Cuddapah Basin, South India. *Total Environ. Res. Themes* **2023**, *8*, 100069. [CrossRef]
87. Goher, M.E.; Farhat, H.I.; Abdo, M.H.; Salem, S.G. Metal Pollution Assessment in the Surface Sediment of Lake Nasser, Egypt. *Egypt. J. Aquat. Res.* **2014**, *40*, 213–224. [CrossRef]
88. Bineshpour, M.; Payandeh, K.; Nazarpour, A.; Sabzalipour, S. Status, Source, Human Health Risk Assessment of Potential Toxic Elements (PTEs), and Pb Isotope Characteristics in Urban Surface Soil, Case Study: Arak City, Iran. *Environ. Geochem. Health* **2021**, *43*, 4939–4958. [CrossRef] [PubMed]
89. Selvam, S.; Jesuraja, K.; Roy, P.D.; Venkatramanan, S.; Khan, R.; Shukla, S.; Manimaran, D.; Muthukumar, P. Human Health Risk Assessment of Heavy Metal and Pathogenic Contamination in Surface Water of the Punnakayal Estuary, South India. *Chemosphere* **2022**, *298*, 134027. [CrossRef]
90. United States Environmental Protection Agency; Office of Emergency; Remedial Response. *Risk Assessment Guidance for Superfund: Pt. A. Human Health Evaluation Manual*; Office of Emergency and Remedial Response, US Environmental Protection Agency: Washington, DC, USA, 1989; Volume 1.
91. Tokatli, C.; Ustaoğlu, F. Health Risk Assessment of Toxicants in Meriç River Delta Wetland, Thrace Region, Turkey. *Environ. Earth Sci.* **2020**, *79*, 426. [CrossRef]
92. Mahato, M.K.; Singh, P.K.; Tiwari, A.K.; Singh, A.K. Risk Assessment Due to Intake of Metals in Groundwater of East Bokaro Coalfield, Jharkhand, India. *Expo. Health* **2016**, *8*, 265–275. [CrossRef]
93. Kumar, V.; Parihar, R.D.; Sharma, A.; Bakshi, P.; Singh Sidhu, G.P.; Bali, A.S.; Karaouzas, I.; Bhardwaj, R.; Thukral, A.K.; Gyasi-Agyei, Y.; et al. Global Evaluation of Heavy Metal Content in Surface Water Bodies: A Meta-Analysis Using Heavy Metal Pollution Indices and Multivariate Statistical Analyses. *Chemosphere* **2019**, *236*, 124364. [CrossRef]
94. United States Environmental Protection Agency. *Regional Screening Level (RSL) Summary Table*; United States Environmental Protection Agency: Washington, DC, USA, 2013.
95. Das Sharma, S. Risk Assessment via Oral and Dermal Pathways from Heavy Metal Polluted Water of Kolleru Lake—A Ramsar Wetland in Andhra Pradesh, India. *Environ. Anal. Health Toxicol.* **2020**, *35*, e2020019. [CrossRef]
96. Kumar, R.N.; Solanki, R.; Kumar, J.I.N. Seasonal Variation in Heavy Metal Contamination in Water and Sediments of River Sabarmati and Kharicut Canal at Ahmedabad, Gujarat. *Environ. Monit. Assess.* **2013**, *185*, 359–368. [CrossRef]
97. Giri, S.; Singh, A.K. Spatial Distribution of Metal(Loid)s in Groundwater of a Mining Dominated Area: Recognising Metal(Loid) Sources and Assessing Carcinogenic and Non-Carcinogenic Human Health Risk. *Int. J. Environ. Anal. Chem.* **2016**, *96*, 1313–1330. [CrossRef]
98. Gao, B.; Gao, L.; Gao, J.; Xu, D.; Wang, Q.; Sun, K. Simultaneous Evaluations of Occurrence and Probabilistic Human Health Risk Associated with Trace Elements in Typical Drinking Water Sources from Major River Basins in China. *Sci. Total Environ.* **2019**, *666*, 139–146. [CrossRef] [PubMed]
99. Qu, L.; Huang, H.; Xia, F.; Liu, Y.; Dahlgren, R.A.; Zhang, M.; Mei, K. Risk Analysis of Heavy Metal Concentration in Surface Waters across the Rural-Urban Interface of the Wen-Rui Tang River, China. *Environ. Pollut.* **2018**, *237*, 639–649. [CrossRef]
100. Sinha, D.; Datta, S.; Mishra, R.; Agarwal, P.; Kumari, T.; Adeyemi, S.B.; Kumar Maurya, A.; Ganguly, S.; Atique, U.; Seal, S.; et al. Negative Impacts of Arsenic on Plants and Mitigation Strategies. *Plants* **2023**, *12*, 1815. [CrossRef]
101. Singh, A.; Kostova, I. Health Effects of Heavy Metal Contaminants Vis-à-Vis Microbial Response in Their Bioremediation. *Inorganica Chim. Acta* **2024**, *568*, 122068. [CrossRef]
102. Obasi, P.N.; Akudinobi, B.B. Potential Health Risk and Levels of Heavy Metals in Water Resources of Lead–Zinc Mining Communities of Abakaliki, Southeast Nigeria. *Appl. Water Sci.* **2020**, *10*, 184. [CrossRef]
103. Mubeen, S.; Ni, W.; He, C.; Yang, Z. Agricultural Strategies to Reduce Cadmium Accumulation in Crops for Food Safety. *Agriculture* **2023**, *13*, 471. [CrossRef]
104. Zulfiqar, U.; Haider, F.U.; Ahmad, M.; Hussain, S.; Maqsood, M.F.; Ishfaq, M.; Shahzad, B.; Waqas, M.M.; Ali, B.; Tayyab, M.N.; et al. Chromium Toxicity, Speciation, and Remediation Strategies in Soil-Plant Interface: A Critical Review. *Front. Plant Sci.* **2023**, *13*, 1081624. [CrossRef] [PubMed]
105. Fahim, R.; Cheng, L.; Mishra, S. Structural and Functional Perspectives of Carbon Filter Media in Constructed Wetlands for Pollutants Abatement from Wastewater. *Chemosphere* **2023**, *345*, 140514. [CrossRef]
106. Hassan, M.U.; Lihong, W.; Nawaz, M.; Ali, B.; Tang, H.; Rasheed, A.; Zain, M.; Alqahtani, F.M.; Hashem, M.; Qari, S.H.; et al. Silicon a Key Player to Mitigate Chromium Toxicity in Plants: Mechanisms and Future Prospective. *Plant Physiol. Biochem.* **2024**, *208*, 108529. [CrossRef]
107. Samantara, M.K.; Padhi, R.K.; Sowmya, M.; Kumaran, P.; Satpathy, K.K. Heavy Metal Contamination, Major Ion Chemistry and Appraisal of the Groundwater Status in Coastal Aquifer, Kalpakkam, Tamil Nadu, India. *Groundw. Sustain. Dev.* **2017**, *5*, 49–58. [CrossRef]
108. Mesquita, A.F.; Gonçalves, F.J.; Gonçalves, A.M. The Lethal and Sub-Lethal Effects of Fluorinated and Copper-Based Pesticides—A Review. *Int. J. Environ. Res. Public Health* **2023**, *20*, 3706. [CrossRef] [PubMed]
109. Pant, R.; Mathpal, N.; Chauhan, R.; Singh, A.; Gupta, A. A Review of Mercury Contamination in Water and Its Impact on Public Health. In *Mercury Toxicity Mitigation: Sustainable Nexus Approach*; Springer Nature: Cham, Switzerland, 2024; pp. 93–115. [CrossRef]
110. Vácha, R. Heavy Metal Pollution and Its Effects on Agriculture. *Agronomy* **2021**, *11*, 1719. [CrossRef]

111. Zheng, X.; Fang, Y.; Lin, J.; Luo, J.; Li, S.; Aschner, M.; Jiang, Y. Signal Transduction Associated with Mn-Induced Neurological Dysfunction. *Biol. Trace Elem. Res.* **2023**, *202*, 1–12. [CrossRef]
112. Mustafa, A.; Zulfiqar, U.; Mumtaz, M.Z.; Radziemska, M.; Haider, F.U.; Holatko, J.; Hammershmiedt, T.; Naveed, M.; Ali, H.; Kintl, A.; et al. Nickel (Ni) Phytotoxicity and Detoxification Mechanisms: A Review. *Chemosphere* **2023**, *328*, 138574. [CrossRef]
113. Kazberuk, W.; Szulc, W.; Rutkowska, B. Use Bottom Sediment to Agriculture—Effect on Plant and Heavy Metal Content in Soil. *Agronomy* **2021**, *11*, 1077. [CrossRef]
114. Menšík, L.; Hlisnikovský, L.; Nerušil, P.; Kunzová, E. Comparison of the Concentration of Risk Elements in Alluvial Soils Determined by pXRF In Situ, in the Laboratory, and by ICP-OES. *Agronomy* **2021**, *11*, 938. [CrossRef]
115. Piwowarska, D.; Kiedrzyńska, E.; Jaszczyszyn, K. A Global Perspective on the Nature and Fate of Heavy Metals Polluting Water Ecosystems, and Their Impact and Remediation. *Crit. Rev. Environ. Sci. Technol.* **2024**, *54*, 1436–1458. [CrossRef]
116. Duan, M.; Li, T.; Liu, B.; Yin, S.; Zang, J.; Lv, C.; Zhao, G.; Zhang, T. Zinc Nutrition and Dietary Zinc Supplements. *Crit. Rev. Food Sci. Nutr.* **2023**, *63*, 1277–1292. [CrossRef]
117. Oueld Lhaj, M.; Moussadek, R.; Mouhir, L.; Mdarhri Alaoui, M.; Sanad, H.; Iben Halima, O.; Zouahri, A. Assessing the Evolution of Stability and Maturity in Co-Composting Sheep Manure with Green Waste Using Physico-Chemical and Biological Properties and Statistical Analyses: A Case Study of Botanique Garden in Rabat, Morocco. *Agronomy* **2024**, *14*, 1573. [CrossRef]
118. Das, S.; Nag, S.K. Application of Multivariate Statistical Analysis Concepts for Assessment of Hydrogeochemistry of Groundwater—A Study in Suri I and II Blocks of Birbhum District, West Bengal, India. *Appl. Water Sci.* **2017**, *7*, 873–888. [CrossRef]
119. Kumar, M.; Das, N.; Tripathi, S.; Verma, A.; Jha, P.K.; Bhattacharya, P.; Mahlknecht, J. Global Co-Occurrences of Multi-(Emerging)-Contaminants in the Hotspots of Arsenic Polluted Groundwater: A Pattern of Menace. *Curr. Opin. Environ. Sci. Health* **2023**, *34*, 100483. [CrossRef]
120. Shi, J.; Zhao, D.; Ren, F.; Huang, L. Spatiotemporal Variation of Soil Heavy Metals in China: The Pollution Status and Risk Assessment. *Sci. Total Environ.* **2023**, *871*, 161768. [CrossRef] [PubMed]
121. Wang, C.-C.; Zhang, Q.-C.; Yan, C.-A.; Tang, G.-Y.; Zhang, M.-Y.; Ma, L.Q.; Gu, R.-H.; Xiang, P. Heavy Metal(loid)s in Agriculture Soils, Rice, and Wheat across China: Status Assessment and Spatiotemporal Analysis. *Sci. Total Environ.* **2023**, *882*, 163361. [CrossRef] [PubMed]
122. George, S.E.; Wan, Y. Microbial Functionalities and Immobilization of Environmental Lead: Biogeochemical and Molecular Mechanisms and Implications for Bioremediation. *J. Hazard. Mater.* **2023**, *457*, 131738. [CrossRef] [PubMed]
123. Pradhan, B.; Chand, S.; Chand, S.; Rout, P.R.; Naik, S.K. Emerging Groundwater Contaminants: A Comprehensive Review on Their Health Hazards and Remediation Technologies. *Groundw. Sustain. Dev.* **2023**, *20*, 100868. [CrossRef]
124. Kükrer, S.; Mutlu, E. Assessment of Surface Water Quality Using Water Quality Index and Multivariate Statistical Analyses in Saraydüzü Dam Lake, Turkey. *Environ. Monit. Assess.* **2019**, *191*, 71. [CrossRef]
125. Ward, J.H., Jr. Hierarchical Grouping to Optimize an Objective Function. *J. Am. Stat. Assoc.* **1963**, *58*, 236–244. [CrossRef]
126. Stefan, D.S.; Bosomoiu, M.; Teodorescu, G. The Behavior of Polymeric Pipes in Drinking Water Distribution System—Comparison with Other Pipe Materials. *Polymers* **2023**, *15*, 3872. [CrossRef]

Disclaimer/Publisher's Note: The statements, opinions and data contained in all publications are solely those of the individual author(s) and contributor(s) and not of MDPI and/or the editor(s). MDPI and/or the editor(s) disclaim responsibility for any injury to people or property resulting from any ideas, methods, instructions or products referred to in the content.